

## OPEN ACCESS

## EDITED BY

Jun-Mo Kim,  
Chung-Ang University, South Korea

## REVIEWED BY

Nouman Amjad,  
Islamia University of  
Bahawalpur, Pakistan  
Tansol Park,  
Chung-Ang University, South Korea

## \*CORRESPONDENCE

Matthew A. Scott  
mascott@cvm.tamu.edu

<sup>†</sup>These authors share senior authorship

## SPECIALTY SECTION

This article was submitted to  
Livestock Genomics,  
a section of the journal  
Frontiers in Veterinary Science

RECEIVED 02 August 2022

ACCEPTED 25 August 2022

PUBLISHED 26 September 2022

## CITATION

Scott MA, Woolums AR, Karisch BB,  
Harvey KM and Capik SF (2022) Impact  
of preweaning vaccination on host  
gene expression and antibody titers in  
healthy beef calves.  
*Front. Vet. Sci.* 9:1010039.  
doi: 10.3389/fvets.2022.1010039

## COPYRIGHT

© 2022 Scott, Woolums, Karisch,  
Harvey and Capik. This is an  
open-access article distributed under  
the terms of the [Creative Commons  
Attribution License \(CC BY\)](https://creativecommons.org/licenses/by/4.0/). The use,  
distribution or reproduction in other  
forums is permitted, provided the  
original author(s) and the copyright  
owner(s) are credited and that the  
original publication in this journal is  
cited, in accordance with accepted  
academic practice. No use, distribution  
or reproduction is permitted which  
does not comply with these terms.

# Impact of preweaning vaccination on host gene expression and antibody titers in healthy beef calves

Matthew A. Scott<sup>1\*†</sup>, Amelia R. Woolums<sup>2</sup>, Brandi B. Karisch<sup>3</sup>,  
Kelsey M. Harvey<sup>4</sup> and Sarah F. Capik<sup>5,6†</sup>

<sup>1</sup>Veterinary Education, Research, and Outreach Center, Texas A&M University and West Texas A&M University, Canyon, TX, United States, <sup>2</sup>Department of Pathobiology and Population Medicine, Mississippi State University, Mississippi State, MS, United States, <sup>3</sup>Department of Animal and Dairy Sciences, Mississippi State University, Mississippi State, MS, United States, <sup>4</sup>Prairie Research Unit, Mississippi State University, Prairie, MS, United States, <sup>5</sup>Texas A&M AgriLife Research, Texas A&M University System, Amarillo, TX, United States, <sup>6</sup>Department of Veterinary Pathobiology, School of Veterinary Medicine and Biomedical Sciences, Texas A&M University, College Station, TX, United States

The impact of preweaning vaccination for bovine respiratory viruses on cattle health and subsequent bovine respiratory disease morbidity has been widely studied yet questions remain regarding the impact of these vaccines on host response and gene expression. Six randomly selected calves were vaccinated twice preweaning (T1 and T3) with a modified live vaccine for respiratory pathogens and 6 randomly selected calves were left unvaccinated. Whole blood samples were taken at first vaccination (T1), seven days later (T2), at revaccination and castration (T3), and at weaning (T4), and utilized for RNA isolation and sequencing. Serum from T3 and T4 was analyzed for antibodies to BRSV, BVDV1a, and BHV1. Sequenced RNA for all 48 samples was bioinformatically processed with a HISAT2/StringTie pipeline, utilizing reference guided assembly with the ARS-UCD1.2 bovine genome. Differentially expressed genes were identified through analyzing the impact of time across all calves, influence of vaccination across treatment groups at each timepoint, and the interaction of time and vaccination. Calves, regardless of vaccine administration, demonstrated an increase in gene expression over time related to specialized proresolving mediator production, lipid metabolism, and stimulation of immunoregulatory T-cells. Vaccination was associated with gene expression related to natural killer cell activity and helper T-cell differentiation, enriching for an upregulation in Th17-related gene expression, and downregulated genes involved in complement system activity and coagulation mechanisms. Type-1 interferon production was unaffected by the influence of vaccination nor time. To our knowledge, this is the first study to evaluate mechanisms of vaccination and development in healthy calves through RNA sequencing analysis.

## KEYWORDS

beef calves, vaccination, preweaned calves, bovine respiratory disease, immunity, RNA sequencing (RNA-Seq), T-cell, inflammation

## Introduction

Vaccination remains one of the most important tools for controlling bovine respiratory disease (BRD) in beef calves (1). Increasing adaptive immunity against known pathogens is the goal of vaccination; however, the presentation of antigens to the immune system elicits multiple cascading events within an animal as part of both innate and adaptive immunity. The most commonly measured indicators of adaptive immunity are serum antibody titers to specific pathogens of interest. Although useful, antibody titers have some limitations including multiple samples must be taken for accurate diagnosis of infection by endemic respiratory agents, and sufficient time must pass for the immune system to respond adequately (2, 3). One alternative to antibody titers is to evaluate differential gene expression to identify markers that indicate immune competency, immune responsiveness, and/or predict future immunity to those pathogens. However, knowledge gaps remain regarding the impact of vaccination on gene expression and how that gene expression may correlate with the development of adaptive immunity.

Although commercially available vaccines have been evaluated and approved by the USDA APHIS Center for Veterinary Biologics for purity, safety, potency, and efficacy, the requirements for efficacy studies are often quite different than the conditions under which the vaccine will be used in the field. While challenge studies can be very useful tools (4), they do not accurately model natural bovine respiratory disease and are often done with seronegative calves that have not been exposed to any pathogens or stressors. Strict protocols and timing of administration are also followed. In contrast, beef producers often use vaccines at different intervals from the label, in animals with a variety of backgrounds and nutritional, immune function, or passive transfer status, and often in the face of bacterial or viral exposure or other stressors (5). These differences can make it difficult to achieve the efficacy seen in the tightly controlled approval studies and raises the question whether vaccines, as commercially employed, are influencing rates of morbidity and performance in a consistent manner. To answer this question, the cattle industry needs additional research on these vaccines as they are employed in natural field conditions and the impact they have on cattle health, performance, and immune function.

Given this background, our objective was to explore differences in host gene expression in calves that were vaccinated preweaning with a modified live vaccine for respiratory pathogens or not *via* time-course transcriptomics, and to pair those data with antibody titers and health records. These data will support exploration of associations and generation of hypotheses regarding the immune response to vaccination that may influence future research and use of vaccines in preweaned beef calves.

## Materials and methods

### Animal use and study enrollment

All animal use and procedures were approved by the Mississippi State University Animal Care and Use Committee (IACUC protocol #19-169) and carried out in accordance with relevant IACUC and agency guidelines and regulations. This study was carried out in accordance with Animal Research: Reporting of *In Vivo* Experiments (ARRIVE) guidelines (6).

Eighty-four bull calves were enrolled in a split plot design study to evaluate the impact of different management strategies on BRD morbidity, mortality, and performance (7). Animals were randomly assigned to whole plot (VAX or NOVAX) which were housed in 6 pastures during the cow-calf phase with no nose-to-nose contact. They were also randomly assigned to split plot level treatment of being directly transported to Texas for backgrounding after weaning (DIRECT) or sent to an auction market and then an order buyer facility for 3 days prior to transport to Texas for backgrounding (AUCTION); this event occurred after the timepoint T4, described below. All animals were visually assessed each day for signs of BRD and/or other disease by trained university employees and detailed health histories were kept on each calf. The observed signs of BRD were assigned a severity score of 0–4, adapted from the scoring system previously described by Holland et al. (8).

Calves were evaluated at four time points, described as T1, T2, T3, and T4. At T1, calves were vaccinated with 2 ml Pyramid 5 (Boehringer Ingelheim Animal Health) subcutaneously (VAX) or given 2 ml 0.9% saline subcutaneously (NOVAX) (median age = 107 days). Additionally, calves were tested *via* ear notch ELISA to evaluate PI status at T1; no PI positive calves were found. At T2, or 7 days post-vaccination (median age = 114 days), all calves were weighed and sampled. At T3 VAX calves were again administered (revaccinated with) 2 ml Pyramid 5 subcutaneously and NOVAX calves were given 2 ml 0.9% saline subcutaneously (median age = 183 days); all calves were castrated by knife with no analgesia on T3. All calves also received 5 ml of a multivalent clostridial bacterin-toxoid (Covexin 8, Merck Animal Health) subcutaneously at time point T1 and T3). All calves were handled so that no contact between vaccinated and non-vaccinated calves would occur. Calves were abruptly weaned at T4 (median age = 230 days) and entered the next phase of the study where they were kept in their original pastures in Mississippi for 3 days before being transported directly from Mississippi to Texas for backgrounding (DIRECT) or sent to an auction market where they stayed in a pen not in contact with other cattle for approximately 6 h, and then were transported for housing at an order buyer facility for 3 days prior to transport to Texas (AUCTION) Non-study calves from other sources were housed at the order buyer facility at the same time as the study calves, but they were not mixed with the study calves. In Texas (samples not evaluated in this study), calves were

kept in one of 12 pens corresponding to their original random assignment to whole and split plot treatments ( $n = 3$  pens of each pair of treatments). Whole blood was collected from all calves into Tempus RNA blood tubes (Applied Biosystems) and into serum tubes *via* jugular venipuncture immediately prior to first vaccination (T1), seven days post-vaccination (T2), immediately prior to vaccine booster administration and castration (T3), and at time of abrupt weaning (T4; 47 days post-booster). Overall, there were 7 days between T1 and T2, 70 days between T2 and T3, and 47 days between T3 and T4.

Twelve calves that remained clinically unaffected by BRD during the cow-calf and backgrounding phases of production were selected for RNA sequencing *via* stratified random sampling within the calves that remained healthy throughout the study within each backgrounding pen which resulted in 1 calf selected per backgrounding pen ( $n = 3$  VAX/DIRECT,  $n = 3$  NOVAX/DIRECT,  $n = 3$  VAX/AUCTION, and  $n = 3$  NOVAX/AUCTION). A total of 48 blood samples across the four time points were analyzed for whole blood transcriptomes. Metadata for all selected calves are found in [Supplementary material 1](#).

## Antibody titers

Serum collected at T3 and T4 was stored at  $-20^{\circ}\text{F}$  before analysis at the University of Georgia's Athens Veterinary Diagnostic Laboratory. Serum neutralizing antibodies were assayed for bovine herpesvirus-1 (BHV-1), bovine viral diarrhea virus type 1a (BVDV1a), bovine respiratory syncytial virus (BRSV), and parainfluenza-3 virus (PI-3) per SOP # Ser013. Resulting titer levels for these antibodies are found in [Supplementary material 1](#) and is limited to descriptive analysis only due to the small number of calves ( $n = 12$ ).

## Average daily gain

Differences in average daily gain between T1 and T4 were evaluated *via* generalized linear mixed effect models estimated *via* restricted pseudolikelihood with the Kenward-Rodgers adjustment for degrees of freedom in SAS 9.4. The model included vaccination status as a fixed effect and a random intercept for backgrounding pastures. Differences in least square means are reported and a cutoff of  $p \leq 0.05$  was used to determine significance.

## Next-generation RNA sequencing and bioinformatic data processing

Total RNA isolation, quality control, sequencing library preparation, and sequencing was performed by the Texas

A&M University Institute for Genome Sciences and Society (TIGSS; College Station, TX, USA). Total RNA was isolated with Tempus Spin RNA Isolation Kit (Applied Biosystems), based on manufacturer's instructions. Total RNA from each sample was analyzed for RNA concentration and integrity with a Qubit 2.0 Fluorometer (ThermoFisher) and an Agilent 2,200 Bioanalyzer (Agilent), respectively; all RNA samples were of high quality (RIN: 7.8–9.5; mean = 8.8, s.d. = 0.3) and concentrations ( $\text{ng}/\mu\text{L}$ : 84.1–380.0; mean = 222.4, s.d. = 71.4). Library preparation for mRNA was performed with the TruSeq Stranded mRNA Library Prep Kit (Illumina), following manufacturer's instruction. Paired-end sequencing for 150 base pair read fragments was performed on an Illumina NovaSeq 6000 analyzer (v1.7+; S4 reagent kit v1.5) in one flow cell lane.

Quality assessment of reads was performed with FastQC v0.11.9<sup>1</sup> and MultiQC v1.12 (9), and read pair trimming for unambiguous base calls, adaptors, and retained minimum read length of 28 bases was performed with Trimmomatic v0.39 (10). Trimmed reads were mapped and indexed to the bovine reference genome assembly ARS-UCD1.2 with HISAT2 v2.2.1 (11). Sequence Alignment/Map (SAM) files were converted to Binary Alignment Map (BAM) files, prior to transcript assembly, with Samtools v1.14 (12). Transcript assembly and gene-level expression estimation for differential expression analysis was performed with StringTie v2.1.7 (13), as described by Pertea et al. (14). All sequencing data produced in this study are available at the National Center for Biotechnology Information Gene Expression Omnibus (NCBI-GEO), under the accession number GSE205004.

## Differential gene expression analysis

Gene-level count matrices were processed and analyzed in RStudio, using R v4.1.2. Samples were classified by vaccination group and time point, where raw gene counts were processed and filtered by procedures described by Chen et al. (15). Any gene with a minimum total count above 100 and a count-per-million (CPM) of 0.2 in at least twelve samples was retained for further analysis. Post filtering, the complete dataset was considered non-sparse, and therefore normalized for differential expression analysis with the trimmed mean of M-values method (TMM) (16). Tagwise dispersion estimates of gene counts were supplied into the Bioconductor package glmmSeq v0.1.0<sup>2</sup> for negative binomial mixed effect modeling of gene counts. The following linear mixed-effect model was fitted to account for time points and vaccination group as

1 <https://www.bioinformatics.babraham.ac.uk/projects/fastqc/>

2 <https://github.com/KatrionaGoldmann/glmmSeq>

fixed effects, and housing (pasture) and individual ID as random effects:

$$\text{Model: } \sim \text{Timepoint} * \text{Vaccine} * \text{Timepoint} : \text{Vaccine} \\ + (1|\text{Pasture}) + (1|\text{ID})$$

Model adaptation allowed for the assessment of differentially expressed genes (DEGs) across timepoints, vaccine groups, and the interactions between timepoints and vaccine group, where *p*-values were adjusted for false discovery rates (FDR) with the Benjamini-Hochberg method; genes were considered significantly expressed with an  $\text{FDR} \leq 0.05$ . Pairwise comparisons for DEGs between each vaccination groups at every time point and within each vaccination group across each time point was performed with edgeR v3.36.0 (15, 17), fitting genes under generalized linear model (GLM) framework and employing quasi-likelihood F-tests (QLF); pairwise gene comparisons were considered significant with an  $\text{FDR} \leq 0.10$ .

## Dimensional reduction and unsupervised clustering analyses

Heatmap, principal component, and clustering analyses were performed with all filtered and log<sub>2</sub> count-per-million (log<sub>2</sub>CPM) values of TMM-normalized gene counts between all 48 samples. Heatmap and exploratory clustering analysis of samples, with respect to vaccination, time points, and individual IDs, were performed with the Bioconductor package pheatmap v1.0.12,<sup>3</sup> utilizing Canberra distances and Pearson correlation coefficients for unsupervised hierarchical clustering of samples and DEGs, respectively. Specifically, *z*-scores were calculated and utilized for heatmap analysis from log<sub>2</sub>CPM values of normalized (TMM) expression values. Gene expression was grouped into 48 distinct clusters with the *k*-means algorithm embedded within pheatmap; the number of clusters was determined from the Elbow method. High dimensional data exploration and reduction *via* principal component analysis (PCA) was conducted with the Bioconductor package PCAtools v2.0.0,<sup>4</sup> utilizing a correlation matrix; normalized gene counts were processed through mean centering and variance scaling. A scree plot was generated to determine the number of principal components (PCs) to retain for analysis, utilizing Elbow and Horn's parallel analysis methods (18). A Spearman's rank correlation matrix of retained PCs was constructed with metadata components from all samples, which included individual identification (ID), birthweight, age of animal for each sample (Age), housing pen at Mississippi (Pasture), vaccination group (Vaccine), sampling time point for each sample (Timepoint), and the slope of weight gain over time

starting at birth (i.e., growth rate; GR); correlations were considered significant with an  $\text{FDR} \leq 0.10$ . To determine genes which were driving the variation seen among each significantly correlated PC, a loadings plot was generated with the top/bottom 2% retained variables across each component loading range. A PCA biplot was constructed from the PCs with significant correlation to vaccination groups; data ellipses were calculated from multivariate *t*-distributions and encompassed 80% confidence levels of expressional *t*-distribution across each time point.

## Functional enrichment analyses of DEGs

Differentially expressed genes were analyzed for functional enrichment of gene ontology (GO) terms, Reactome pathways, and KEGG pathways with KOBAS-i (19) (accessed May 2, 2022), utilizing hypergeometric testing and Benjamini-Hochberg adjusted *p*-values ( $\text{FDR} \leq 0.05$ ). Functional enrichment of DEGs were analyzed in three separate analyses: (1) DEGs shared between time points in both glmmSeq and QLF testing of vaccinated and non-vaccinated calves (i.e., shared genes between glmmSeq-timepoints, QLF Vax T1vsT2, and QLF Novax T1vsT2), (2) DEGs identified between vaccination groups across each time point by both glmmSeq-vaccination and QLF testing (i.e., glmmSeq-Vaccine and Vax vs. Novax at T1), removing DEGs identified by method #1, and (3) DEGs solely identified in glmmSeq analysis of Timepoint: Vaccine interactions; this approach allowed for the independent assessment of functional enrichment influenced by calf development (i.e., time) and vaccine administration. Enriched GO terms and pathways were evaluated for directionality (increased or decreased) based on log<sub>2</sub> fold changes of associated DEGs. Clustering and visualization of enriched KEGG terms was performed with the embedded enrichment visualization tool within KOBAS-i, utilizing edge (correlation) thresholds of 0.40 and top *n* clusters set to 8; more information regarding the embedded enrichment visualization tool framework is provided by Bu et al. (19).

## Results

### Antibody titers and average daily gain

Comparison of antibody titers indicated calves were likely naturally infected with BRSV and PI-3, because antibody titers to these agents increased between T3 and T4 in both vaccinated and non-vaccinated calves. Given the small number of calves evaluated, this somewhat clouds our ability to detect the effect of vaccination using serology of samples collected at only two timepoints. However, vaccinated calves appeared to respond well to MLV vaccination as indicated by the BVDV1a titer response (Supplementary material 1). Average daily gain between T1 and T4 was not significantly different ( $p = 0.31$ ) between the

<sup>3</sup> <https://CRAN.R-project.org/package=pheatmap>

<sup>4</sup> <https://github.com/kevinblighe/PCAtools>

VAX (model-adjusted least square mean 1.89 lbs) and NOVAX (model-adjusted least square mean 2.13 lbs) groups.

## Differential gene expression patterns and enriched biological mechanisms

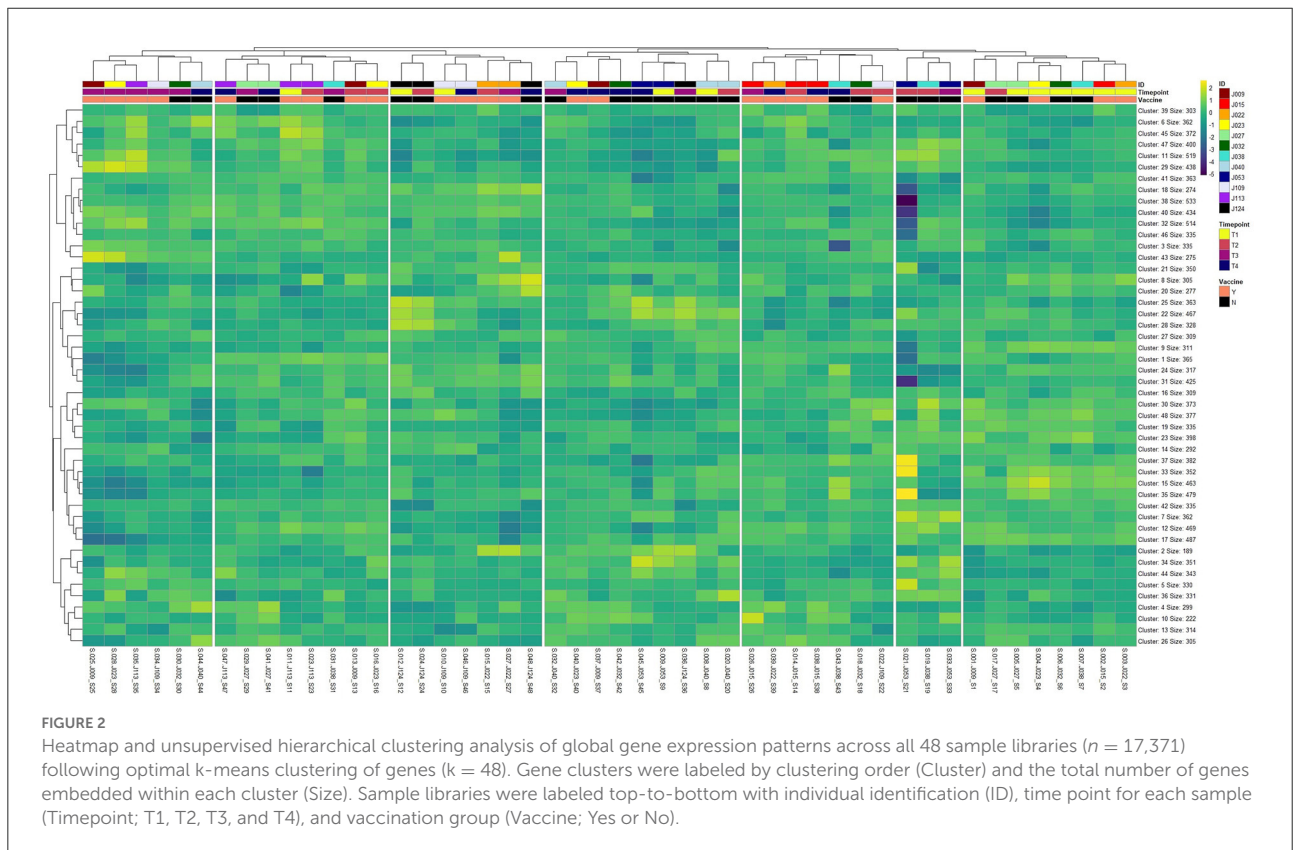
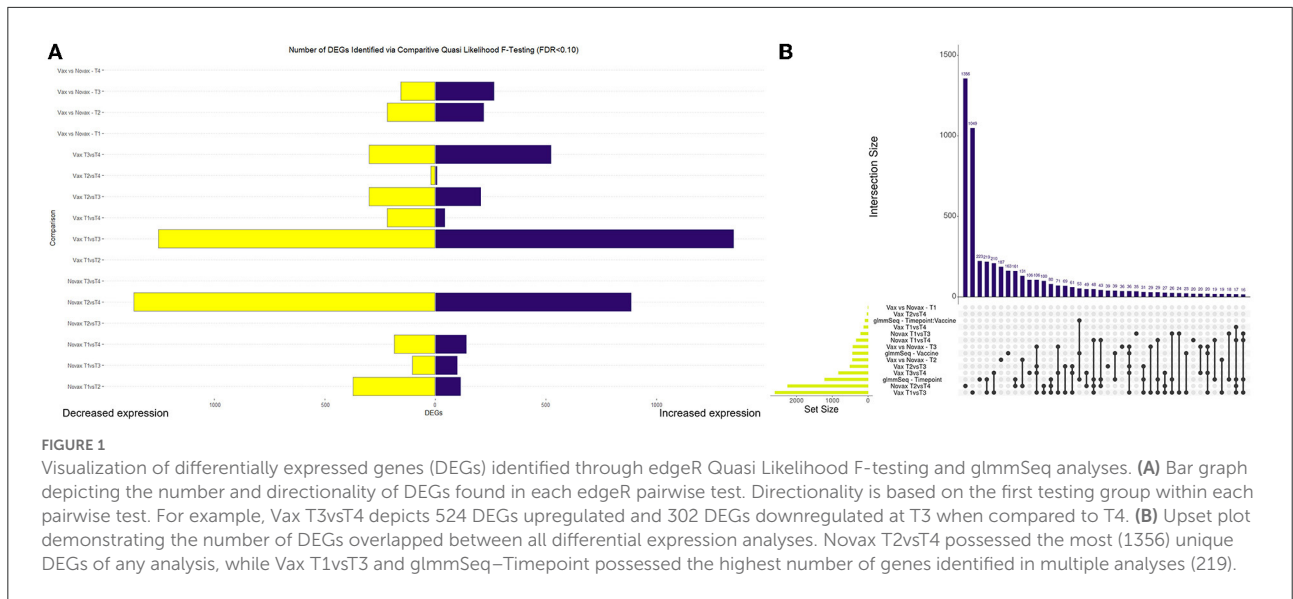
Read mapping and alignment of the 48 transcriptomes to the ARS-UCD1.2 bovine reference genome resulted in an overall mapping rate average of 95.50% (s.d. = 0.96%). In total, gene-level alignment resulted in a total of 33,310 unique features, with a median library size of 41,089,614 (s.d. = 4,111,721) (Supplementary Figure 1). Pre-processing and filtering of low expression values resulted in a total of 17,371 genes used for downstream analyses (Supplementary Table 2). Analysis of genes from glmmSeq resulted in 1213, 435, and 85 DEGs when evaluating time, vaccination, and the interaction of time and vaccination, respectively (Supplementary Table 3). Comparative analyses for DEGs between vaccination groups and time points was conducted with edgeR GLM-QLF testing. Analysis of the NOVAX group over time yielded a total of 3,271 DEGs across six comparisons (Supplementary material 4). Analysis of the VAX group over time yielded a total of 4,085 DEGs across six comparisons (Supplementary material 5). Analysis of each time point between the VAX and NOVAX groups yielded a total of 861 DEGs across four comparisons (Supplementary material 6). Visualization of the number and directionality of DEGs identified from GLM-QLF testing and overlapping of DEGs from glmmSeq and edgeR QLF analyses, are found in Figure 1.

Heatmap and unsupervised clustering analysis, seen in Figure 2, demonstrated that the majority of calves ( $n = 7$ ) were highly similar in global gene expression prior to vaccine administration (T1; right side). Time of sampling (Timepoint) emerged as a considerable factor in determining distinction between groups (Vaccine) and individual calves (ID), as the majority of samples on the left side of the heatmap (i.e., furthest from the T1 samples) were at time of vaccine boosting (T3) and weaning (T4). Several individuals (J015, J022, J027, J053, J109, J113, J124) demonstrated high self-similarity in global gene expression between time points.

Multidimensionality analysis and visualization of global gene expression patterns *via* PCA is found in Figure 3. Utilizing both the elbow method and Horn's parallel analysis, a total of 14 principal components (PCs) were determined as optimal for demonstrating explained variation across the 48 transcriptomes; the first 14 PCs retained 70.15% of the variance within the data (Figure 3A). Pairwise plotting of selective PCs (Figures 3B,C) was performed with those PCs which demonstrated significant correlations with timepoints and/or vaccination status (Figure 3D). The first PC, accounting for 14.20% of the total explained variance, was positively

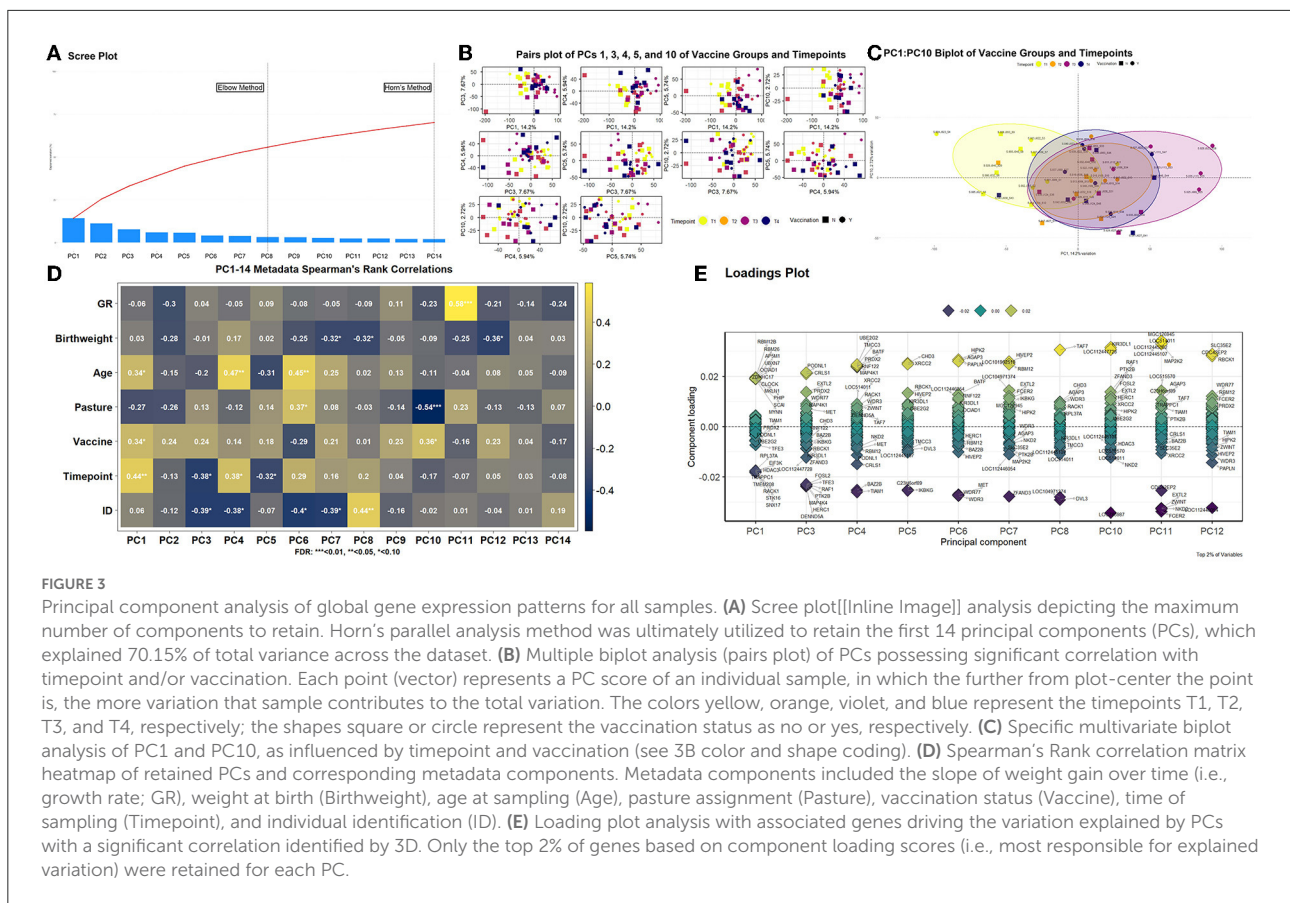
correlated with Age ( $r = 0.34$ , FDR < 0.10), Vaccine ( $r = 0.34$ , FDR < 0.10), and Timepoint ( $r = 0.44$ , FDR < 0.05). Two PCs, PC3 and PC4, accounting for 7.67 and 5.94% of total explained variance, respectively, demonstrated significant correlations with Timepoint but not Vaccine; PC3 demonstrated negative correlation with Timepoint ( $r = -0.38$ , FDR < 0.10) and ID ( $r = -0.39$ , FDR < 0.10) and PC4 demonstrated positive correlation with Timepoint ( $r = 0.38$ , FDR < 0.10) and Age ( $r = 0.47$ , FDR < 0.05), confounded by ID ( $r = -0.38$ , FDR < 0.10). Accounting for 5.74% of total explained variance, PC5 possessed significant negative correlation with Timepoint ( $r = -0.32$ , FDR < 0.10). While confounded by Pasture ( $r = -0.54$ , FDR < 0.01), PC10, accounting for 2.72% of total explained variance, possessed significant positive correlation with Vaccine ( $r = 0.36$ , FDR < 0.10). Notably, the strongest correlation found within this analysis was between PC11, accounting for 2.33% of total explained variance, and GR ( $r = 0.58$ , FDR < 0.01). The resulting pairwise plotting of PCs 1, 3, 4, 5, and 10 demonstrated relative overlapping of all samples at T1, with increasing dissimilarity of samples over time (Figure 3B). A biplot with statistical ellipses (multivariate C.I. = 80.00%) of the two PCs with significant correlation with Vaccine (PC1 and PC10) demonstrated high dissimilarity between timepoints T1 and T3, with relative high overlap of timepoints T2 and T4, with T3 variation driven by vaccinated calves J009, J022, J023, and J113 (Figure 3C). Genes driving the variation among each PC possessing significant metadata correlations are found in Figure 3E. Specifically, genes influencing variation within PC1 and PC10 (i.e., correlated PCs with Vaccination) include *AP5M1*, *CLOCK*, *EIF3K*, *HDAC3*, *MKLN1*, *MYNN*, *OCIAD1*, *PHIP*, *RACK1*, *RBM12B*, *RBM26*, *RPL37A*, *SNX17*, *STK16*, *TMEM208*, *TRAPPC1*, *UBXN7*, and *ZDHHC17* in PC1 and *KIR3DL1*, *LOC112447728*, and *LOC786987* in PC10, respectively. Those PCs having significant correlation with Timepoint, and not Vaccine (PC3, PC4, and PC5), possessed variance-driving genes which overlapped with glmmSeq-timepoint findings; *BATF*, *EXTL2*, *PRDX2*, *RNF122*, *TIAM1*, and *TMCC3* were identified in both PC3-5 loadings plots and glmmSeq-timepoint analysis.

Analysis of GO terms, KEGG pathways, and Reactome pathways of genes identified between glmmSeq-timepoints and edgeR QLF testing within both vaccination groups across time allowed for the assessment of enriched processes and pathways at three specific timepoint comparisons: (1) T1 vs. T3, (2) T1 vs. T4, and (3) T2 vs. T4 (Supplementary material 7). Shared DEGs from T1 vs. T3 comparisons enriched for 88 GO terms and 72 functional pathways. These GO terms were related to zinc ion binding, cytokine-mediated signaling, specifically interleukin-12, gene expression regulation, regulation to inflammatory response, including negative regulation of I-kappaB kinase/NF-kappaB signaling, and fatty acid metabolism and biosynthesis. Enriched pathways included the immune system (both innate and acquired immunity) retrograde endocannabinoid signaling,



interleukin-4/13 signaling, glucose metabolism, glucagon signaling, TP53 expressional and degradation regulation, and the biosynthesis of specialized proresolving mediators (SPMs), including SPMs derived from both docosahexaenoic acid (DHA) and eicosapentaenoic acid (EPA). These GO terms

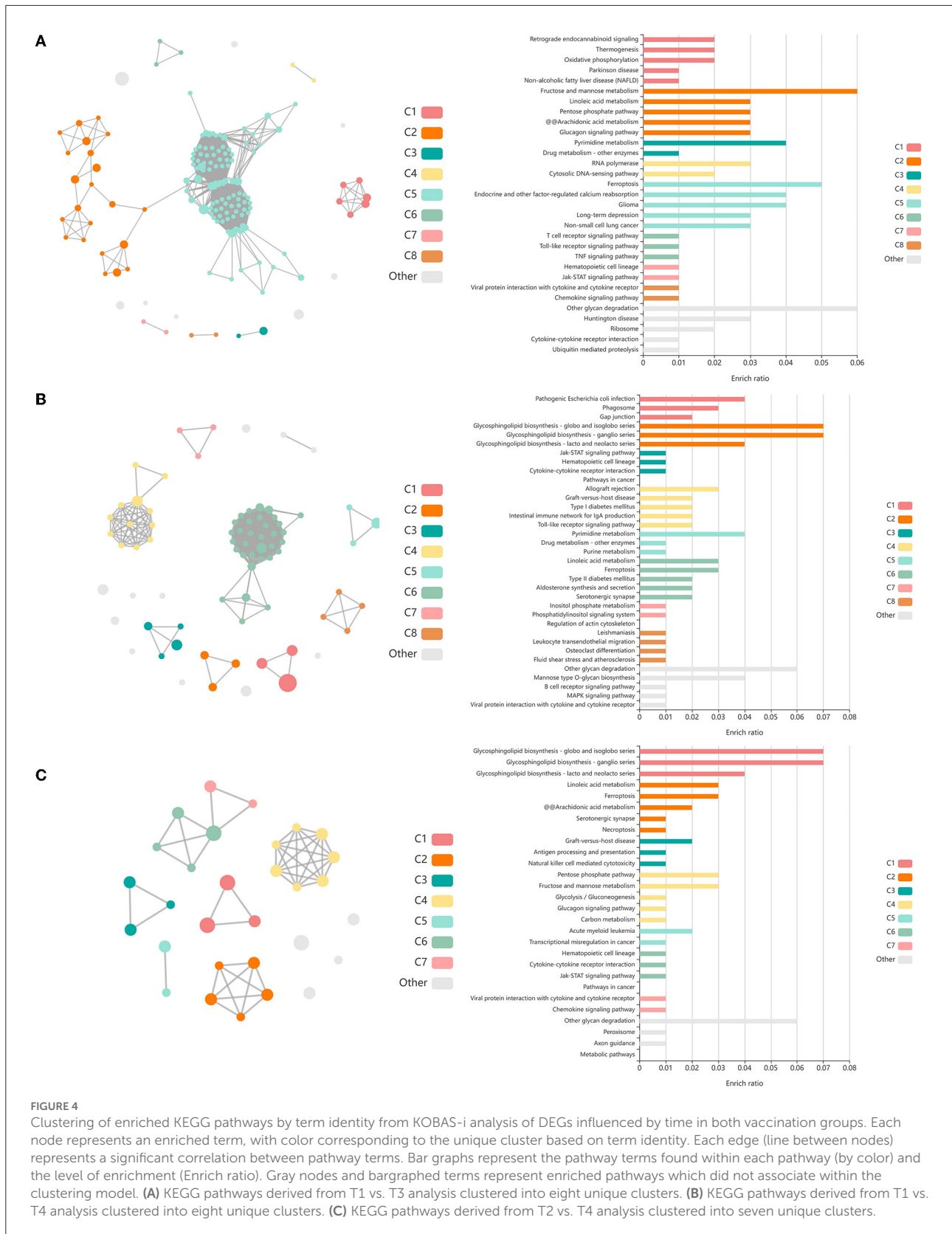
and pathways were primarily enriched by the following DEGs: *ADAMTS12*, *ALOX15*, *ALOX5*, *CFL1*, *CPT1A*, *FBP1*, *FSCN1*, *IL5RA*, *LOC100297044* (*CCL14*), *LOC615278* (*TRIM39*), *LOC789732* (*CD300C*), *MIF*, *OTUD7B*, *PEG10*, *PIKFYVE*, *PLP2*, *POLR2L*, *PPP2R1A*, *PRKCG*, *PYGM*, *TK1*, and *TP53*.



Shared DEGs from T1 vs. T4 comparisons enriched for 34 GO terms and 35 functional pathways. These GO terms were related to inflammatory response, cytokine-mediated signaling, magnesium ion binding, cellular response to oxidative stress, positive regulation of autophagy, T-cell co-stimulation, and actin/microtubule organization and development. Enriched pathways included the acquired immune system, interleukin signaling, cellular stress response, CD28 co-stimulation and signaling, and gap junction trafficking and regulation. These GO terms and pathways were primarily enriched by the following DEGs: *ALOX15*, *CD80*, *HMGAI*, *HSPB8*, *IL17REL*, *IL5RA*, *LOC100297044* (*CCL14*), *LOC533307* (*LRRK2*), *LOC789732* (*CD300LD*), *MAP3K8*, *NCF2*, *SLC7A11*, *TUBB*, *TUBB3*, and *ZC3H12A*. Shared DEGs from T2 vs. T4 comparisons enriched for 94 GO terms and 29 functional pathways. These GO terms were related to inflammatory and cytokine-mediated response, specifically including interleukin-17 receptor activity, MHC class I protein complex binding, response to mercury and magnesium ions, antigenic stimuli and macrophage differentiation, and fatty acid metabolism and biosynthesis. Enriched pathways included cellular metabolism involving fructose, mannose, pyruvate, and lipid metabolism, cytokine-cytokine receptor interaction, and the biosynthesis of specialized proresolving mediators (SPMs), including SPMs derived from

both docosahexaenoic acid (DHA) and eicosapentaenoic acid (EPA). These GO terms and pathways were primarily enriched by the following DEGs: *ALOX15*, *CEBPE*, *DECR2*, *FBP1*, *IL17REL*, *IL5RA*, *LOC100297044* (*CCL14*), *LOC788694* (*KLRC1*), and *SLC7A11*. Visualization of the enriched KEGG pathway terms is found in Figure 4. Expressional trends of DEGs identified in all three timepoint comparisons between the two vaccination groups (*ALOX15*, *IL5RA*, *IL17REL*, *LOC100297044* (*CCL14*), and *SCL7A11*) are found in Figure 5.

A total of 435 genes were identified by glmmSeq-Vaccination to be differentially expressed (Supplementary material 3), with 109 unique DEGs identified by overlapping glmmSeq-Vaccination and GLM-QLF testing results, post-removal of DEGs identified in Timepoint evaluation (Supplementary material 8). Specifically, a total of one, 24, and 92 DEGs were identified between vaccination groups at timepoints T1, T2, and T3, respectively; no genes were found to be differentially expressed between vaccinated and non-vaccinated calves at T4 (Supplementary material 8). Only one DEG was identified at T1 (*HEXDC*; increased in Vaccinated) between vaccinated and non-vaccinated calves, therefore possessed no enriched GO terms nor pathways. Shared DEGs identified at T2 between vaccinated and non-vaccinated calves enriched for 139 GO terms and 61 functional



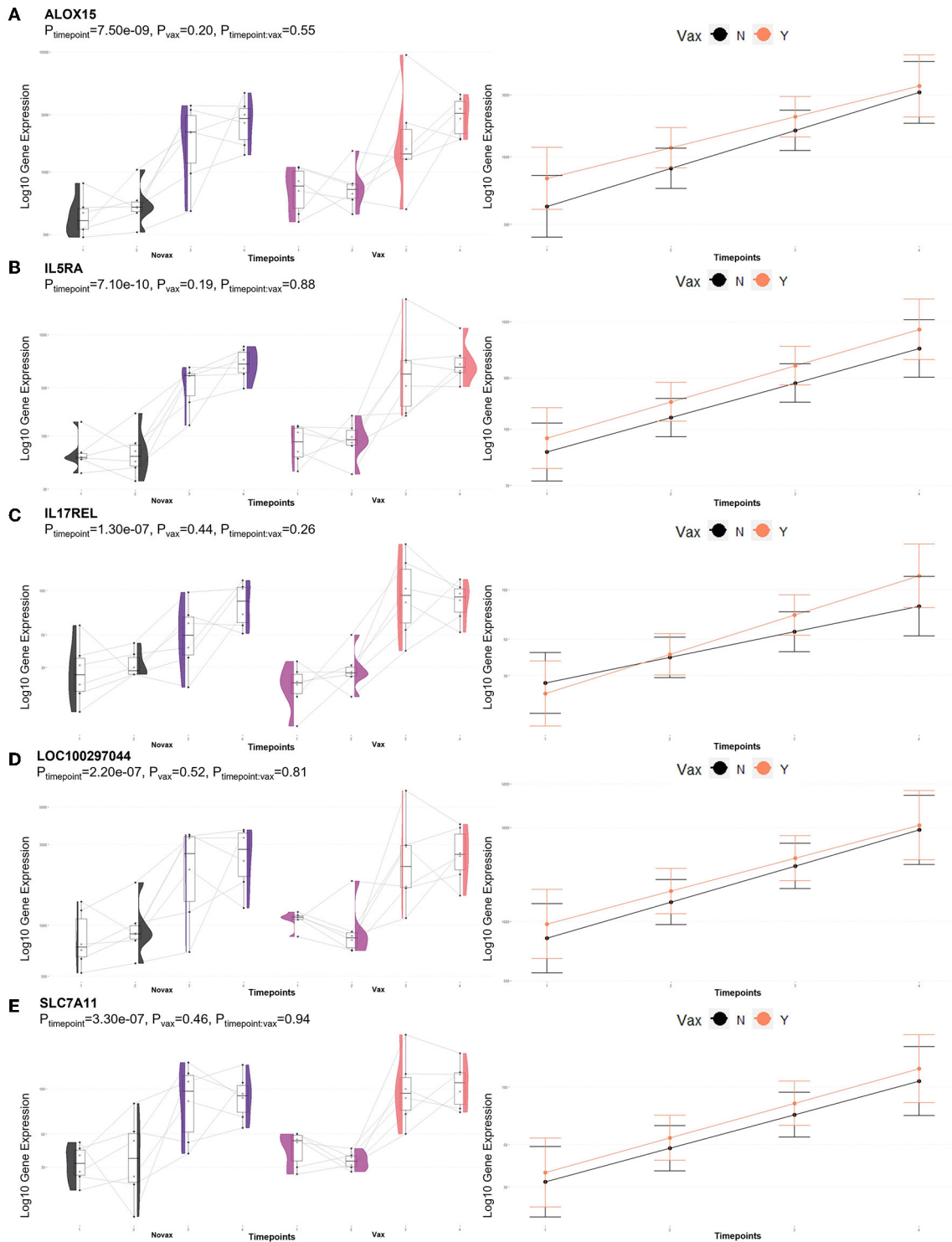
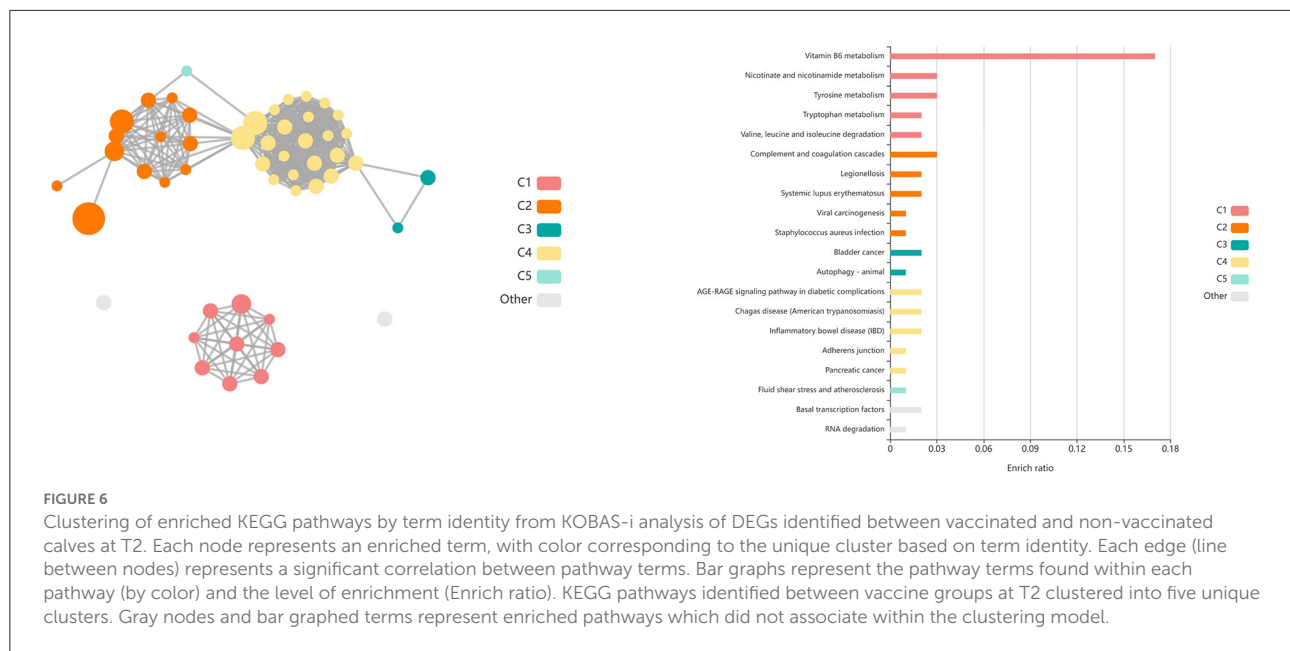


FIGURE 5

Gene pairplots and modeled expression trends of key DEGs found in timepoint analyses. Pairplots (left side) demonstrate the log10 normalized gene expression of each sample across all timepoints, overlapped with a violin plot (depicting numerical distributions by density). Box-and-whisker plots represent median expression values (black line), the first (lower) and third quartiles (boxplot limits), 1.5 times the interquartile ranges (whiskers), and outlier expression levels for each timepoint (points outside whiskers). Modeled expression trends (right side) depict the overall differences between groups over each timepoint. Points represent the mean log10 normalized expression value for each group within a timepoint, and bars represent the standard error of log10 normalized expression for each group; orange represents the vaccinated group and black represents the non-vaccinated group. These plots depict the relative expression and glmSeq level of significance for (A) *ALOX15*, (B) *IL5RA*, (C) *IL17REL*, (D) *LOC100297044* (*CCL14*), and (E) *SLC7A11*.

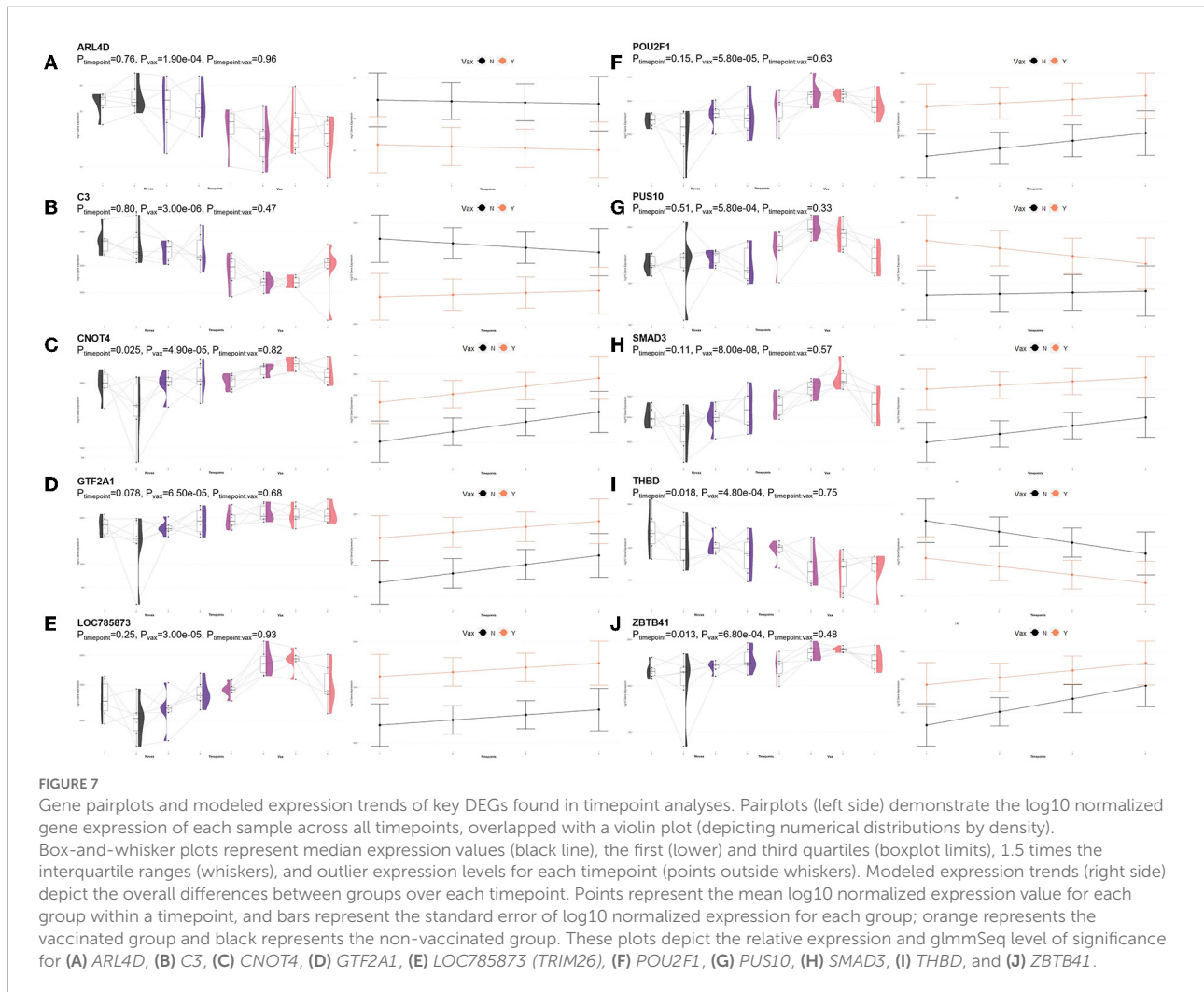


pathways. These GO terms were related to immune response and regulation (increased in Vaccinated), T-cell activation (increased in Vaccinated), metal ion binding (increased in Vaccinated), positive transcriptional regulation and protein processing (increased in Vaccinated), cellular proliferation and maintenance (increased in Vaccinated), complement activity (decreased in Vaccinated), and apoptotic clearance and phagocytosis (decreased in Vaccinated). Enriched pathways included the immune system and cytokine signaling, including interleukin-37 signaling (increased in Vaccinated), complement and coagulation cascades (decreased in Vaccinated), enhanced transcriptional activity, largely involving RNA polymerase II (increased in Vaccinated), and vitamin B6 metabolism (decreased in Vaccinated). These GO terms and pathways were primarily enriched by the following DEGs: *ARL4D*, *C3*, *CNOT4*, *GTF2A1*, *LOC785873* (*TRIM26*), *POU2F1*, *PUS10*, *SMAD3*, *THBD*, and *ZBTB41*. Visualization of the enriched KEGG pathways is found in Figure 6. Expressional trends of the aforementioned DEGs contributing to these GO terms and pathways are found in Figure 7.

Shared DEGs identified at T3 between vaccinated and non-vaccinated calves enriched for 71 GO terms and 25 functional pathways. These GO terms were related to neutrophil degranulation (increased in Vaccinated), antigen processing and presentation (increased in Vaccinated), ubiquitin protein binding and positive regulation (increased in Vaccinated), nuclear protein importing and response to protein folding (increased in Vaccinated), heat shock protein binding, specifically to Hsp70 and Hsp90 (increased in Vaccinated), T-cell activation (increased in Vaccinated), cellular response to interleukin-7 (increased in Vaccinated),

and the positive regulation to ATPase activity (increased in Vaccinated). Enriched pathways included transcription activation (increased in Vaccinated), endocytosis and antigen processing and presentation (increased in Vaccinated), neutrophil degranulation (increased in Vaccinated), and cellular response to heat stress, including the regulation of HSF1-mediated heat shock response, Hsp90 chaperone cycle for steroid hormone receptors, and HSF1-dependent transactivation (all increased in Vaccinated). These GO terms and pathways were primarily enriched by the following DEGs: *AHSA2*, *BANP*, *C3*, *CACYBP*, *CCT2*, *DNAJA4*, *DNAJB1*, *DNAJB4*, *HIST1H3G*, *HSP90AB1*, *HSPA14*, *HSPA1A*, *HSPA4*, *HSPA6*, *HSPD1*, *HSPH1*, *KAT2A*, *MDM4*, *NUTF2*, *PTPRB*, *RAB11FIP3*, *RCHY1*, *SMAD3*, *STIP1*, *SYMPK*, *TOMM34*, *TRAF2*, *ZFAND2A*, *ZFP28*, and *ZNF473*. Visualization of the enriched KEGG pathway terms is found in Figure 8. Expressional trends of the DEGs primarily involved in immune mediated and heat shock response associated GO terms and pathways (*DNAJB1*, *DNAJB4*, *HSP90AB1*, *HSPA14*, *HSPA1A*, *HSPA4*, *HSPA6*, *HSPD1*, *HSPH1*, and *TRAF2*) are found in Figure 9.

A total of 85 DEGs were identified by glmmSeq when evaluating the interaction between Vaccination and Timepoints, which enriched for 13 GO terms and six functional pathways (Supplementary material 9). These GO terms were related to extracellular space, actin filament organization, cytoplasmic vesicles, copper ion binding, and natural killer cell activation and mediated cytotoxicity. Enriched pathways included small molecule transport, immunoregulatory interactions between lymphoid and non-lymphoid cells, plasma lipoprotein remodeling, natural killer cell mediated cytotoxicity, tyrosine



metabolism, and DAP12 interactions. Visualization of the enriched KEGG pathway terms is found in Figure 10. Expressional trends of the DEGs primarily involved in immunoregulatory and natural killer cell associated GO terms and pathways (*AOC3*, *DCT*, *LOC100852061* (*KIR2DS2*), *LOC101905165* (*NKG2D*), *LOC112441504* (*ULBP3*), and *LOXL4*) is found in Figure 11.

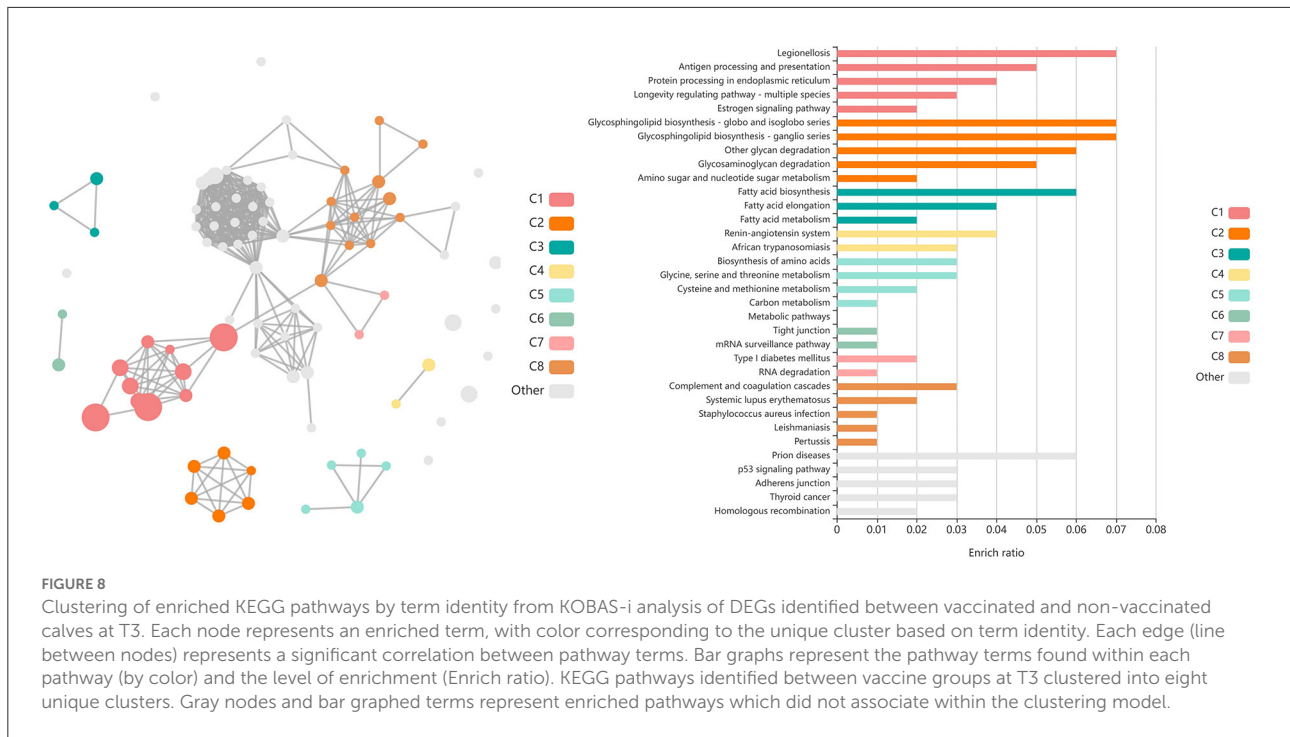
## Discussion

### Use of modified live viral respiratory vaccines in beef cattle production systems

The use of modified live viral (MLV) vaccines in beef cattle backgrounding and feeding operations remains one of the leading practices in managing risk of BRD in cattle populations (1). Multiple recent reviews have evaluated the peer-reviewed

literature regarding the use of various vaccines for respiratory pathogens in beef cattle (20–22). However, vaccination is not always helpful (23) and questions remain regarding which cattle are most likely to benefit from vaccination and which may not. Assessment of the transcriptome may reveal new pathways that will explain why vaccination appears to prevent disease in certain situations but not others. The significance of some of the differences in observed gene expression between VAX and NOVAX calves is not yet clear, but provides a foundation for future studies to determine how multiple components of the immune response change following vaccination. To our knowledge, there is no comparable data set available.

Although variable in terms of individual efficacy, several studies suggest that vaccinating herds of cattle with MLV vaccines reduces herd-level risk of BRD-associated morbidity and mortality and is associated with improved weight gain overtime (i.e., production) (24–27). Our study was limited to a small subset of calves that remained clinically healthy



which may have influenced the subsequent lack of difference in performance.

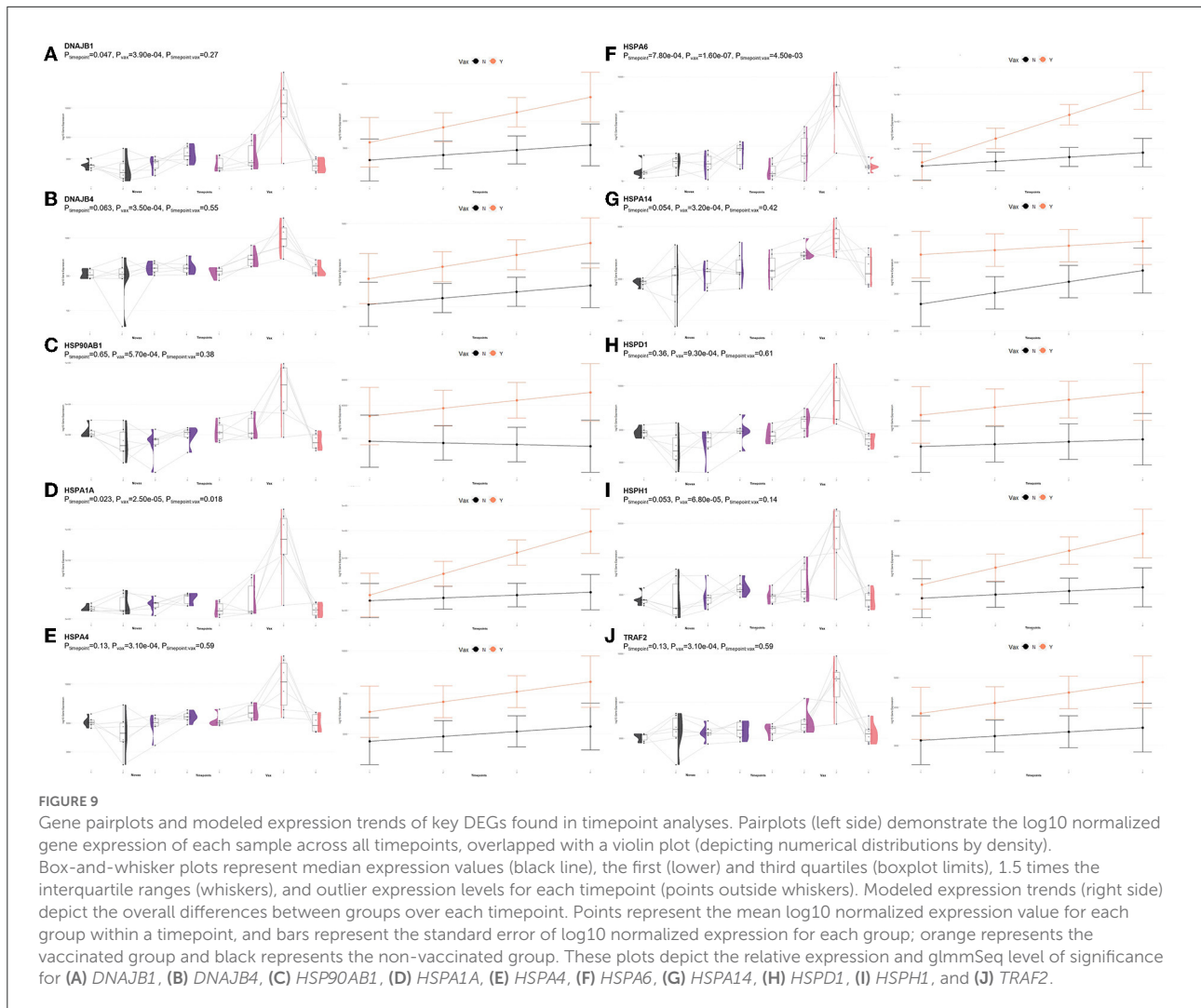
For years, responses to vaccination have been measured *via* serology (4), and occasionally, cell-mediated immune responses (20). Such studies usually describe only a small number of outcomes of a vast and diverse network of interactions that influence health vs. disease. While we attempted to assess serum neutralizing titer responses to the viruses we vaccinated against, the timing of sample collection was not optimized to find peak titer responses. Additionally, it is important to note that in this study the MLV was administered differently than the label directions indicated. The current label for Pyramid 5 (28) does not indicate a minimum age requirement or a specific interval or requirement for revaccination of calves. However, administering a booster vaccination, especially when the primary vaccination was given to animals under 6 months of age, is common industry practice and according to current knowledge would be helpful in initiating a protective immune response. Our serology results indicated that the calves responded to our vaccination strategy as expected but that there was likely a natural exposure to PI-3 and BRSV in the herd. The lack of differential gene expression at T4 between VAX and NOVAX calves is further supported by the titer data at T4. This may be due to the length of time between sampling points T3 and T4, but our data suggest both VAX and NOVAX individuals, across multiple pens, were exposed to a potentially non-virulent strain of PI-3 and BRSV sometime between T3 and T4. Furthermore, the similarities in gene expression between the two groups at T4 may be confounded due to this exposure and processing at T3. However, the results

of this study demonstrated that the driver of immunological response and enhanced transcription over time, as influenced by vaccination, was the initial (first) administration.

### Development of clinically healthy cattle is associated with increased specialized proresolving mediator expression, fatty acid and carbohydrate metabolism, and cytokine-mediated immunity

When evaluating the influence of time (i.e., physiological growth) on the gene expression of young calves, three connected mechanisms continually increased over time across all individuals: specialized proresolving mediator (SPM) biosynthesis, fatty acid and carbohydrate metabolism, and chemokine/cytokine mediated enhancement of acquired immunity. Specialized proresolving mediators consist of closely related classes of lipid mediators, derived from the lipoxygenation of arachidonic acid into LXA4 (i.e., lipoxins) (29) or from the metabolism of omega-3 and/or omega-6 essential polyunsaturated fatty acids (i.e., resolvins, protectins, and maresins) (30–32). Collectively, six molecules (*ALOX5*, *ALOX15*, *GPX4*, *HPGD*, *LTA4H*, and *PTGS2*) are directly involved in the biosynthesis of SPMs,<sup>5</sup> of which we identified

<sup>5</sup> <https://reactome.org/PathwayBrowser/#/R-HSA-9018679&DTAB=MT>

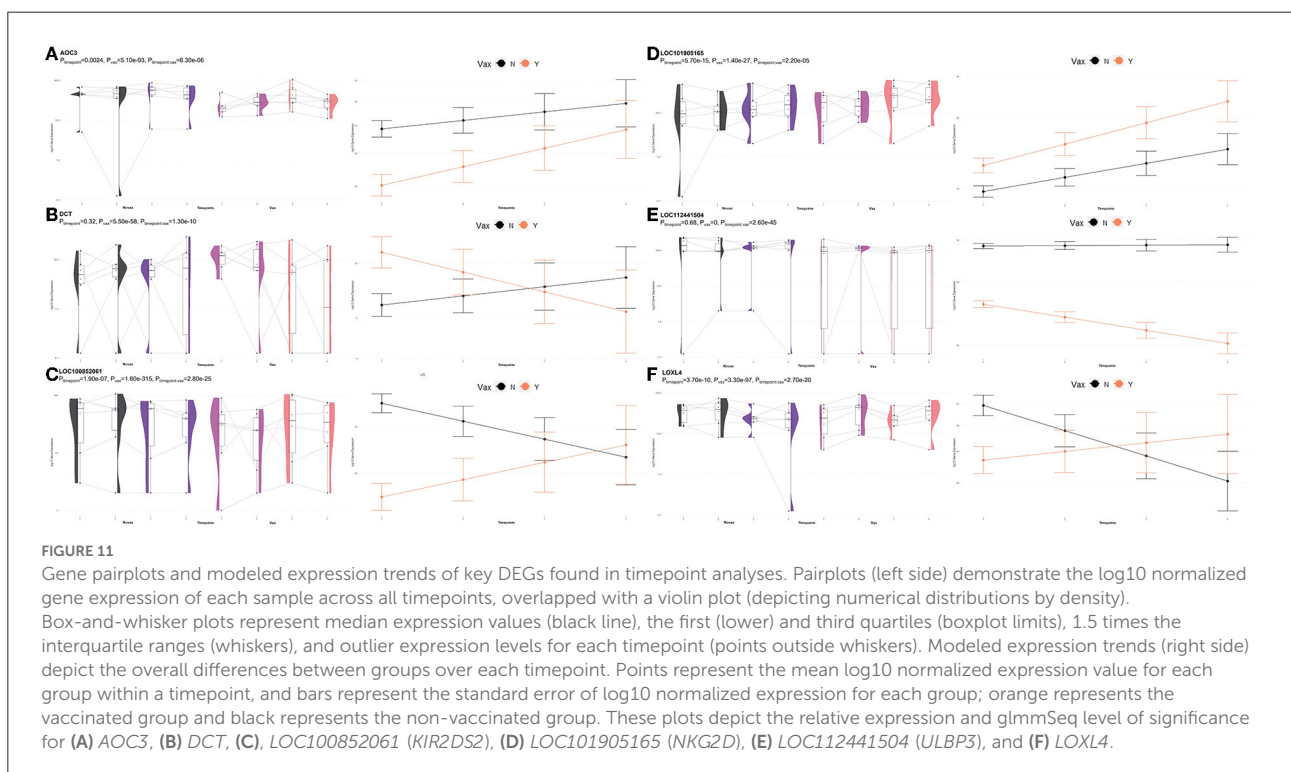
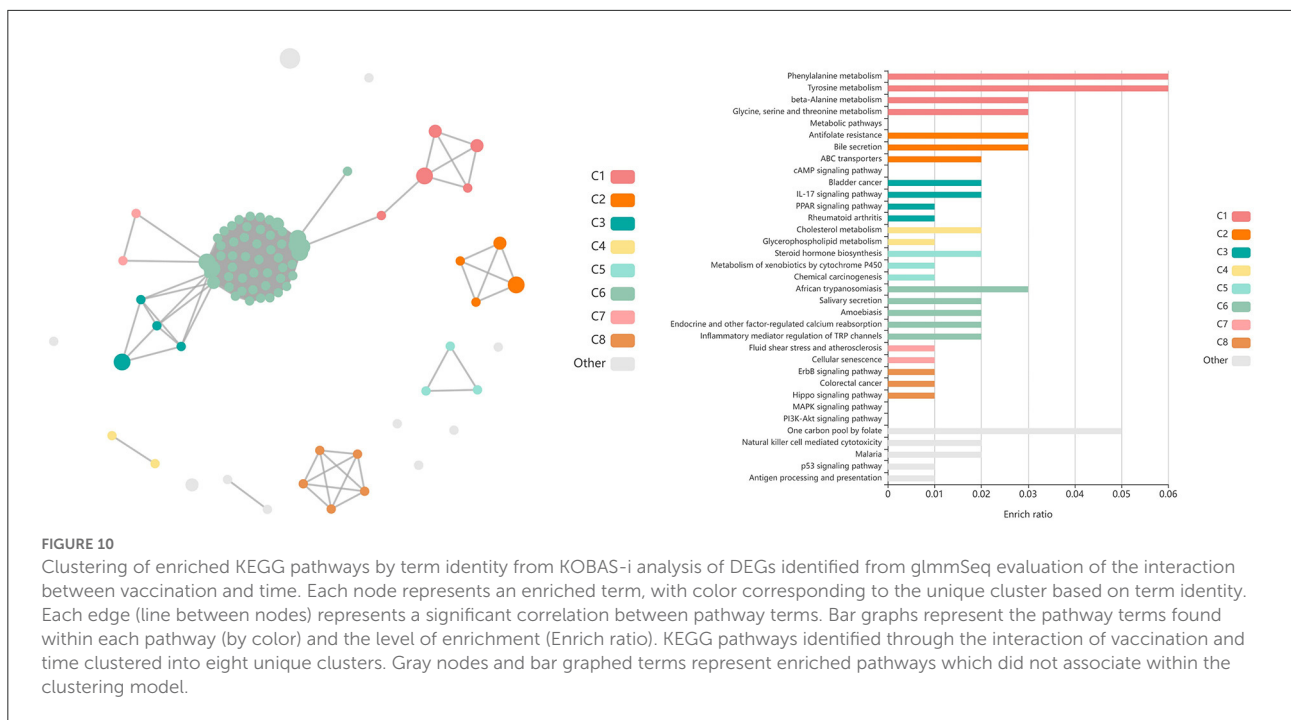


three to be differentially increased in all calves over time (*ALOX5*, *ALOX15*, and *HPGD*); notably, *HPGD* was identified as a differentially expressed in glmmSeq – timepoint, NOVAX T1vT4, VAX T1vT3, and VAX T2vT3. These lipid molecules are profound regulators of both acute and chronic inflammation and are critical in promoting cellular clearance and tissue remodeling in response to respiratory disease (33–36). Recent evidence suggests that, in addition to their ability to resolve inflammatory responses and tissue damage, SPMs are effective modulators of the adaptive immune response, capable of regulating Th1/Th17 differentiation and promoting regulatory T-cell differentiation *via* a non-cytopathic regulatory mechanism (37). Crucially, SPMs are shown to not have an effect on Th2-driven immunity, but enhance antigen presenting cell, specifically dendritic cell, development and functionality (37–39); this aligns with our findings indicating a gradual increase in gene expression related to SPM production and immunoregulatory T-cells. This is additionally supported by the enrichment of CD28 co-stimulation and signaling,

and the enhancement of *CTLA4* and *CD80* with associated cytokine production (*IL5RA*, *IL17REL*) over time (40–44). Furthermore, several of these specific genes, namely *ALOX15*, *LOC100297044* (*CCL14*), *HPGD*, and *IL5RA*, have been identified as DEGs increased in expression at facility arrival in cattle that remain clinical healthy within high-risk populations, compared to cattle that develop BRD (45–49). Collectively, this may represent immunological development and mechanisms of immunocompetence which can serve a protective role against BRD-induced inflammation when calves are placed in post-weaned feeding systems.

### Vaccination induces a controlled inflammatory response linked with Th17/natural killer cell activity

Evaluation of host expression influenced by vaccination, excluding genes and mechanisms affected solely by time,



demonstrated an increase in mechanisms associated with antigen presentation, metal ion binding, molecular chaperone activity, and lymphoid cell activity, and a decrease in mechanisms associated with complement and apoptotic debris clearance. First, through PCA of global expression trends,

we discovered genes driving variation in PCs with significant correlation with vaccination. Specifically, we identified the genes *CLOCK*, *HDAC3*, *KIR3DL1*, *RACK1*, and *SNX17* to be key drivers of differences associated with vaccination, which are involved in regulating the activity and differentiation of

T-cells and natural killer cells. *CLOCK*, in conjunction with *BMAL1*, is a circadian timekeeping protein which interacts with transcriptional regulators, which in turn upregulate genes such as *HDAC3*; this transcriptional network is responsible for the development and differentiation of Th17 cells (50–53). *KIR3DL1*, an immunoglobulin-like receptor expressed by natural killer cells and T-cells (54), is shown to be involved in inhibiting interferon- $\gamma$  secretion and may block the progression of chronic inflammation, seen in research involving ankylosing spondylitis and reactive arthritis (55, 56). *RACK1*, which acts as both an intracellular protein receptor for protein kinase C and as a core ribosomal protein of the 40S subunit, is a key component of T-cell activation and proliferation (57, 58) and loss of *RACK1* has been shown to increase T-cell apoptosis (59). *SNX17* localizes with T-cell receptors and is responsible for preventing T-cell degradation into lysosomes and transporting T-cell receptors to the cell surface, aiding in cellular immune function (60). These findings provide initial evidence that vaccination in young calves influences mechanisms related to the enhanced differentiation and survival of T-cells, natural killer cell activity, and accompanying interleukin-17 response; this coincides with previous research demonstrating vaccination or exposure to viral components mediates a T-helper cell and natural killer cell response (61, 62), which may contribute to protective cell mediated and controlled inflammatory responses (63).

To further explore the influence of vaccination on these calves, we identified DEGs between vaccination groups at each time point, and those found from the interaction between vaccination and time. At T2 (7 days post vaccination), DEGs identified in calves which received a MLV vaccination enriched for two major immune-related mechanisms—the downregulation of complement and coagulation cascades (primarily driven by *C3*), and the upregulation of T-cell-mediated immunity. Complement, a well-organized and highly regulated system of the immune system, is a critical component of host immunity for killing or neutralizing pathogens and maintaining immunological homeostasis (64, 65). While the complement system features three distinct response pathways (classical, alternative, and mannose-binding lectin), all three lead to subsequent *C3* activation (66). Interestingly, the vaccinated group demonstrated a downregulation of *C3* transcription. While complement *C3* is critical for inducing a humoral and cell-mediated response to vaccination and viral infection (67–70), little published information exists relating to the timing and activity levels of induced complement cascades in cattle. Thus, it can be hypothesized that we failed to capture the initial immune responses associated with vaccination within the first few days and are identifying a late feedback mechanism involved in controlling prolonged complement activity. Additionally, research has demonstrated that the complement system appears to be more important for successful immunization in response to polysaccharide-containing vaccines compared to conjugated vaccines (71). Furthermore, we identified DEGs and enriched

mechanisms related to CD4+ T-cell activity, primarily driven by *DAPK2*, *POU2F1*, *SMAD3*, and *LOC785873* (*TRIM26*). *DAPK2* promotes cellular recruitment to sites of inflammation (72) and is highly expressed in activated T-cells, serving a cellular regulatory role during germinal center formation (73). *POU2F1* is a required transcription factor for T-cell response to infection and the development of CD4+ memory T-cells (74–76). *SMAD3* transduces TGF- $\beta$  signaling and controls the development of regulatory T-cells and Th17 cells via signaling networks involving T-cell receptors, TGF- $\beta$ , and interleukin-6 (77, 78). While not directly involved with T-cell activity, *TRIM26* is involved with modulating host antiviral defense and inducing an inflammatory immune response (79–81).

Evaluation of T3 (prior to booster administration; 77 days after initial vaccination) identified DEGs and enriched immunological mechanisms involved in neutrophil degranulation, antigen processing and interleukin-7 response, T-cell activation, transcriptional activity, and heat shock protein activity and binding. At this time point in vaccinated calves compared to non-vaccinated calves, we again observed an increase in the expression of *SMAD3* and *LOC785873* (*TRIM26*), two genes involved in T-cell development and inflammatory defense mechanisms, respectively, and a decrease in *THBD* and *C3*, involved in coagulation (82, 83) and complement activity, respectively. Surprisingly, these genes and associated mechanisms remained significantly enriched at both seven and 77 days post-vaccinated, indicating a possible immune-mediated mechanism or complex induced by MLV vaccination which persists longer than anticipated (>30 days). One unexpected finding at this timepoint was the rapid increase in heat shock protein gene expression in vaccinated calves. There is a great deal of research demonstrating the role of heat shock proteins in vaccination and host immunity/inflammation. Hsp70 enhances immunogenic antigen presentation cell functionality and T-cell proliferation (84). Both Hsp70 and Hsp90 proteins are shown to activate dendritic cells and direct naïve helper T-cell priming through designated interactions with antigen presenting cell surface receptors (85, 86) and stimulating inflammatory cytokine production via CD14-mediated chaperoning (87–89). *HSPD1* initiates interferon-beta production through interactions with interferon regulatory factor 3 (*IRF3*) (90) and is associated with both leukocyte and lymphocyte tissue infiltration (91). Furthermore, both Hsp70 and Hsp90 promote Th17 gene expression and proliferation and are involved in interleukin-17-mediated inflammation (92–94). This collectively indicates a stimulation of heat shock protein-mediated inflammation and helper T-cell, possibly Th17, promotion via modified live viral vaccination. However, this mechanism was only upregulated at T3. How long and where in time this mechanism becomes upregulated through viral vaccination could not be fully elucidated by this study and additional research is needed.

Our final differential expression evaluation was to determine genes influenced by the interaction of both time and vaccination. Largely, the DEGs identified through this analysis were determined to be involved with immunoregulatory functions *via* natural killer cells. These mechanisms were enriched by three key genes: *LOC101905165* (*NKGD2*), *LOC100852061* (*KIR2DS2*), and *LOC112441504* (*ULBP3*). *NKGD2* serves as a costimulatory transmembrane receptor on natural killer cells, enhancing T-cell receptor activity and subsequent cytotoxic and gamma-delta T-cell function (95–97). *KIR2DS2* is an activating receptor of natural killer cells, which binds to MHC class 1 and enhances natural killer cell-mediated cytotoxicity (98, 99). *ULBP3* is a cellular ligand of natural killer cells which binds to *NKGD2*, serving an immunostimulatory role (100–102). This indicates that the influence of both time and vaccination acts in influencing natural killer cell and cytotoxic responses in calves. Bassi et al. (103) demonstrated that cattle naturally infected with and displaying clinical signs of bovine papillomavirus possessed an increase in circulating natural killer cells and CD4<sup>+</sup>/CD8<sup>+</sup> ratios, with a related elevation in interleukin-17 levels, when compared to cattle without clinical papillomatosis. Hamilton et al. (104) found that BCG vaccination in neonatal calves induces effector natural killer cells after interactions with dendritic cells, and stimulates their production of type-2 interferon production and interleukin-12.

Another key detail in this study is the lack of differential expression related to type-1 interferon production and response. Research has demonstrated that administration of recombinant and mRNA vaccines against viral pathogens can induce type-1 interferon production, enhancing T-cell response *via* heightened antigen presentation, and further promoting humoral immunity and vaccine-induced antibody production (105–108). Previous research in cattle has demonstrated that type-1 interferon production is strongly induced by viral challenge and is seen as an antiviral defense mechanism (109–112). While type-1 interferon production in human vaccination trials is well documented, it is relatively unknown if ungulates possess a similar immune response. We may have failed to recognize such a response due to the time between sampling points. Further studies assessing additional time points post-vaccination and booster, and focused assessment of peripheral immune cell types and responses, are warranted to better identify and understand the complex interaction of mechanisms related to successful immunization.

This study is, to our knowledge, the first of its kind to describe differential gene expression pathways in calves over the first 7 months of life, and in relation to a commonly used vaccination scheme, in a longitudinal fashion. Our findings indicate that vaccination induces a controlled inflammatory response associated with natural killer cell and, likely, Th17 cell promotion. This is most likely a normal process of antigen presentation and immunological memory within calves, but still constitutes an inflammatory-inducing process. It may be

hypothesized that these induced mechanisms are not effective when calves are placed in high-risk settings, where stress and inflammation are occurring, compared to the low-risk system in which these calves were studied.

## Data availability statement

The data presented in the study are deposited in the National Center for Biotechnology Information Gene Expression Omnibus (NCBI-GEO), accession number GSE205004.

## Ethics statement

The animal study was reviewed and approved by Mississippi State University Animal Care and Use Committee (IACUC protocol #19-169).

## Author contributions

SC, AW, and BK conceived and designed the vaccination study funded by USDA. MS, AW, BK, and KH managed the live animal project and collected samples and metadata for analysis. MS and SC coordinated diagnostics, analyzed the data, and wrote the manuscript. SC, MS, AW, BK, and KH edited the manuscript and approved the final version. All authors agree to be accountable for the content of the work.

## Funding

This project was supported by Agriculture and Food Research Initiative Competitive Grant no. 2019-67015-29845 from the USDA National Institute of Food and Agriculture. Additionally, this project was supported in part by internal funds provided by Texas A&M AgriLife Research and Texas A&M University School of Veterinary Medicine and Biomedical Sciences.

## Acknowledgments

The authors would like to acknowledge Libby Durst, Kalisha Yankey, Will Crosby, and Jane Parish for their assistance with managing the calves and collecting metadata at MSU. We thank Andrew Hillhouse and the staff at the Texas A&M Institute for Genome Sciences and Society for assistance with the RNA sequencing. We would also like to acknowledge Jill Fishburn and Binu Velayudhan at the University of Georgia Athens Diagnostic Lab for their assistance with the serum neutralizing antibody titers.

## Conflict of interest

The authors declare that the research was conducted in the absence of any commercial or financial relationships that could be construed as a potential conflict of interest.

## Publisher's note

All claims expressed in this article are solely those of the authors and do not necessarily represent those of their affiliated organizations, or those of the publisher, the editors and the reviewers. Any product that may be evaluated in this article, or claim that may be made by its manufacturer, is not guaranteed or endorsed by the publisher.

## References

- Wilson BK, Richards CJ, Step DL, Krehbiel CR. Best management practices for newly weaned calves for improved health and well-being. *J Anim Sci.* (2017) 95:2170–82. doi: 10.2527/jas.2016.1006
- Meeusen ENT, Walker J, Peters A, Pastoret P-P, Jungersen G. Current status of veterinary vaccines. *Clin Microbiol Rev.* (2007) 20:489–510. doi: 10.1128/CMR.00005-07
- Savini G, Tittarelli M, Bonfimi B, Zaghini M, Di Ventura M, Monaco F. Serological response in cattle and sheep following infection or vaccination with bluetongue virus. *Vet Ital.* (2004) 40:645–7.
- Callan RJ, editor. Fundamental considerations in developing vaccination protocols. In *American Association of Bovine Practitioners Annual Conference*. Vancouver, Canada (2001).
- Richeson JT, Hughes HD, Broadway PR, Carroll JA. Vaccination management of beef cattle: delayed vaccination and endotoxin stacking. *Vet Clin North Am Food Anim Pract.* (2019) 35:575–92. doi: 10.1016/j.cvfa.2019.07.003
- Percie du Sert N, Hurst V, Ahluwalia A, Alam S, Avey MT, Baker M, et al. The Arrive guidelines 2.0: updated guidelines for reporting animal research. *PLoS Biol.* (2020) 18:e3000410. doi: 10.1371/journal.pbio.3000410
- Capik SF, Amrine DE, White BJ, Larson RL, Woolums AR, Karisch BB, et al. P170 - Impact of management decisions on bovine respiratory disease morbidity and mortality risks. In: *Conference of Research Workers in Animal Diseases*. Chicago, IL (2019).
- Holland BP, Step DL, Burciaga-Robles LO, Fulton RW, Confer AW, Rose TK, et al. Effectiveness of sorting calves with high risk of developing bovine respiratory disease on the basis of serum haptoglobin concentration at the time of arrival at a feedlot. *Am J Vet Res.* (2011) 72:1349–60. doi: 10.2460/ajvr.72.10.1349
- Ewels P, Magnusson M, Lundin S, Käller M. Multiqc: summarize analysis results for multiple tools and samples in a single report. *Bioinformatics.* (2016) 32:3047–8. doi: 10.1093/bioinformatics/btw354
- Bolger AM, Lohse M, Usadel B. Trimmomatic: a flexible trimmer for illumina sequence data. *Bioinformatics.* (2014) 30:2114–20. doi: 10.1093/bioinformatics/btu170
- Kim D, Paggi JM, Park C, Bennett C, Salzberg SL. Graph-based genome alignment and genotyping with hisat2 and hisat-genotype. *Nat Biotechnol.* (2019) 37:907–15. doi: 10.1038/s41587-019-0201-4
- Li H, Handsaker B, Wysoker A, Fennell T, Ruan J, Homer N, et al. The sequence alignment/map format and samtools. *Bioinformatics.* (2009) 25:2078–9. doi: 10.1093/bioinformatics/btp352
- Kovaka S, Zimin AV, Pertea GM, Razaghi R, Salzberg SL, Pertea M. Transcriptome assembly from long-read rna-seq alignments with stringtie2. *Genome Biol.* (2019) 20:278. doi: 10.1186/s13059-019-1910-1
- Pertea M, Kim D, Pertea GM, Leek JT, Salzberg SL. Transcript-level expression analysis of Rna-Seq experiments with hisat, stringtie and ballgown. *Nat Protoc.* (2016) 11:1650–67. doi: 10.1038/nprot.2016.095

## Author disclaimer

Any opinions, findings, conclusions, or recommendations expressed in this publication are those of the author(s) and do not necessarily reflect the view of the U.S. Department of Agriculture nor the internal supporters of this project.

## Supplementary material

The Supplementary Material for this article can be found online at: <https://www.frontiersin.org/articles/10.3389/fvets.2022.1010039/full#supplementary-material>

- Chen Y, Lun AT, Smyth GK. From reads to genes to pathways: differential expression analysis of rna-seq experiments using rsubread and the edgeR quasi-likelihood pipeline. *F1000Res.* (2016) 5:1438. doi: 10.12688/f1000research.8987.2
- Robinson MD, Oshlack A. A scaling normalization method for differential expression analysis of Rna-Seq data. *Genome Biol.* (2010) 11:R25. doi: 10.1186/gb-2010-11-3-r25
- McCarthy DJ, Chen Y, Smyth GK. Differential expression analysis of multifactor Rna-Seq experiments with respect to biological variation. *Nucleic Acids Res.* (2012) 40:4288–97. doi: 10.1093/nar/gks042
- Horn JL. A rationale and test for the number of factors in factor analysis. *Psychometrika.* (1965) 30:179–85. doi: 10.1007/BF02289447
- Bu D, Luo H, Huo P, Wang Z, Zhang S, He Z, et al. Kobas-I: intelligent prioritization and exploratory visualization of biological functions for gene enrichment analysis. *Nucleic Acids Res.* (2021) 49:W317–w25. doi: 10.1093/nar/gkab447
- Chamorro MF, Palomares RA. Bovine respiratory disease vaccination against viral pathogens: modified-live versus inactivated antigen vaccines, intranasal versus parenteral, what is the evidence? *Vet Clin North Am Food Anim Pract.* (2020) 36:461–72. doi: 10.1016/j.cvfa.2020.03.006
- O'Connor AM, Hu D, Totton SC, Scott N, Winder CB, Wang B, et al. A systematic review and network meta-analysis of bacterial and viral vaccines, administered at or near arrival at the feedlot, for control of bovine respiratory disease in beef cattle. *Anim Health Res Rev.* (2019) 20:143–62. doi: 10.1017/S1466252319000288
- Capik SF, Moberly HK, Larson RL. Systematic review of vaccine efficacy against mannheimia haemolytica, pasteurella multocida, and histophilus Somni in North American Cattle. *Bov. Pract.* (2021) 55:125–33. doi: 10.21423/bovine-vol55no2p125-133
- Stokka GL. Prevention of respiratory disease in cow/calf operations. *Vet Clin Food Anim Pract.* (2010) 26:229–41. doi: 10.1016/j.cvfa.2010.04.002
- Schumacher TF, Cooke RF, Brandão AP, Schubach KM, de Sousa OA, Bohnert DW, et al. Effects of vaccination timing against respiratory pathogens on performance, antibody response, and health in feedlot cattle1. *J Anim Sci.* (2018) 97:620–30. doi: 10.1093/jas/sky466
- Step DL, Krehbiel CR, Burciaga-Robles LO, Holland BP, Fulton RW, Confer AW, et al. Comparison of single vaccination versus revaccination with a modified-live virus vaccine containing bovine herpesvirus-1, bovine viral diarrhoea virus (Types 1a and 2a), parainfluenza type 3 virus, and bovine respiratory syncytial virus in the prevention of bovine respiratory disease in cattle. *J Am Vet Med Assoc.* (2009) 235:580–7. doi: 10.2460/javma.235.5.580
- Palomares RA, Givens MD, Wright JC, Walz PH, Brock KV. Evaluation of the onset of protection induced by a modified-live virus vaccine in calves challenge inoculated with Type 1b bovine viral diarrhoea virus. *Am J Vet Res.* (2012) 73:567–74. doi: 10.2460/ajvr.73.4.567

27. Kelling CL, Hunsaker BD, Steffen DJ, Topliff CL, Eskridge KM. Characterization of protection against systemic infection and disease from experimental bovine viral diarrhoea virus type 2 infection by use of a modified-live noncytopathic type 1 vaccine in calves. *Am J Vet Res.* (2007) 68:788–96. doi: 10.2460/ajvr.68.7.788
28. LLC DS. *Pyramid 5 Boehringer Ingelheim Animal Health USA, Inc.* Available from: <https://bayerall.cvspervice.com/product/view/1028246> (accessed July 22, 2022).
29. Levy BD, Clish CB, Schmidt B, Gronert K, Serhan CN. Lipid mediator class switching during acute inflammation: signals in resolution. *Nat Immunol.* (2001) 2:612–9. doi: 10.1038/89759
30. Serhan CN, Hong S, Gronert K, Colgan SP, Devchand PR, Mirick G, et al. Resolvins: a family of bioactive products of omega-3 fatty acid transformation circuits initiated by aspirin treatment that counter proinflammation signals. *J Exp Med.* (2002) 196:1025–37. doi: 10.1084/jem.20020760
31. Serhan CN, Yang R, Martinod K, Kasuga K, Pillai PS, Porter TF, et al. Maresins: novel macrophage mediators with potent antiinflammatory and proresolving actions. *J Exp Med.* (2009) 206:15–23. doi: 10.1084/jem.20081880
32. Serhan CN. Pro-resolving lipid mediators are leads for resolution physiology. *Nature.* (2014) 510:92–101. doi: 10.1038/nature13479
33. Nijmeh J, Levy BD. Lipid-derived mediators are pivotal to leukocyte and lung cell responses in sepsis and ards. *Cell Biochem Biophys.* (2021) 79:449–59. doi: 10.1007/s12013-021-01012-w
34. El Kebir D, József L, Pan W, Wang L, Petasis NA, Serhan CN, et al. 15-Epi-lipoxin a4 inhibits myeloperoxidase signaling and enhances resolution of acute lung injury. *Am J Respir Crit Care Med.* (2009) 180:311–9. doi: 10.1164/rccm.200810-1601OC
35. Levy BD, Kohli P, Gotlinger K, Haworth O, Hong S, Kazani S, et al. Protectin D1 is generated in asthma and dampens airway inflammation and hyperresponsiveness. *J Immunol.* (2007) 178:496–502. doi: 10.4049/jimmunol.178.1.496
36. Luo J, Zhang WY, Li H, Zhang PH, Tian C, Wu CH, et al. Pro-resolving mediator resolvin E1 restores alveolar fluid clearance in acute respiratory distress syndrome. *Shock.* (2022) 57:565–75. doi: 10.1097/SHK.0000000000001865
37. Chiurchiù V, Leuti A, Dallì J, Jacobsson A, Battistini L, Maccarrone M, et al. Proresolving lipid mediators resolvin D1, resolvin D2, and maresin 1 are critical in modulating T cell responses. *Sci Transl Med.* (2016) 8:353ra111. doi: 10.1126/scitranslmed.aaf7483
38. Basil MC, Levy BD. Specialized pro-resolving mediators: endogenous regulators of infection and inflammation. *Nat Rev Immunol.* (2016) 16:51–67. doi: 10.1038/nri.2015.4
39. Rothe T, Gruber F, Uderhardt S, Ipseiz N, Rössner S, Oskolkova O, et al. 12/15-lipoxygenase-mediated enzymatic lipid oxidation regulates dc maturation and function. *J Clin Invest.* (2015) 125:1944–54. doi: 10.1172/JCI78490
40. Walker LS, Sansom DM. The emerging role of Ctla4 as a cell-extrinsic regulator of T cell responses. *Nat Rev Immunol.* (2011) 11:852–63. doi: 10.1038/nri3108
41. Wu B, Jin M, Zhang Y, Wei T, Bai Z. Evolution of the Il17 receptor family in chordates: a new subfamily Il17rel. *Immunogenetics.* (2011) 63:835–45. doi: 10.1007/s00251-011-0554-4
42. Pätzold L, Stark A, Ritzmann F, Meier C, Tschernig T, Reichrath J, et al. Il-17c and Il-17re promote wound closure in a staphylococcus aureus-based murine wound infection model. *Microorganisms.* (2021) 9:1821. doi: 10.3390/microorganisms9091821
43. Hall BM, Hall RM, Tran GT, Robinson CM, Wilcox PL, Rakesh PK, et al. Interleukin-5 (Il-5) therapy prevents allograft rejection by promoting Cd4(+)Cd25(+) T<sub>H</sub>2 regulatory cells that are antigen-specific and express Il-5 receptor. *Front Immunol.* (2021) 12:714838. doi: 10.3389/fimmu.2021.714838
44. Peach RJ, Bajorath J, Naemura J, Leytze G, Greene J, Aruffo A, et al. Both extracellular immunoglobulin-like domains of Cd80 contain residues critical for binding T cell surface receptors Ctl4-4 and Cd28. *J Biol Chem.* (1995) 270:21181–7. doi: 10.1074/jbc.270.36.21181
45. Sun HZ, Srithayakumar V, Jimenez J, Jin W, Hosseini A, Raszek M, et al. Longitudinal blood transcriptomic analysis to identify molecular regulatory patterns of bovine respiratory disease in beef cattle. *Genomics.* (2020) 112:3968–77. doi: 10.1016/j.ygeno.2020.07.014
46. Scott MA, Woolums AR, Swiderski CE, Perkins AD, Nanduri B, Smith DR, et al. Whole blood transcriptomic analysis of beef cattle at arrival identifies potential predictive molecules and mechanisms that indicate animals that naturally resist bovine respiratory disease. *PLoS ONE.* (2020) 15:e0227507. doi: 10.1371/journal.pone.0227507
47. Scott MA, Woolums AR, Swiderski CE, Perkins AD, Nanduri B, Smith DR, et al. Multipopulation transcriptome analysis of post-weaned beef cattle at arrival further validates candidate biomarkers for predicting clinical bovine respiratory disease. *Sci Rep.* (2021) 11:23877. doi: 10.1038/s41598-021-03355-z
48. Scott MA, Woolums AR, Swiderski CE, Thompson AC, Perkins AD, Nanduri B, et al. Use of ncounter mrna profiling to identify at-arrival gene expression patterns for predicting bovine respiratory disease in beef cattle. *BMC Vet Res.* (2022) 18:77. doi: 10.1186/s12917-022-03178-8
49. Scott MA, Woolums AR, Swiderski CE, Finley A, Perkins AD, Nanduri B, et al. Hematological and gene co-expression network analyses of high-risk beef cattle defines immunological mechanisms and biological complexes involved in bovine respiratory disease and weight gain. *bioRxiv.* (2022). doi: 10.1101/2022.02.16.480640 [preprint].
50. Man K, Loudon A, Chawla A. Immunity around the clock. *Science.* (2016) 354:999–1003. doi: 10.1126/science.aah4966
51. Yu X, Rollins D, Ruhn KA, Stubblefield JJ, Green CB, Kashiwada M, et al. Th17 cell differentiation is regulated by the circadian clock. *Science.* (2013) 342:727–30. doi: 10.1126/science.1243884
52. Yang G, Chen L, Grant GR, Paschos G, Song WL, Musiek ES, et al. Timing of expression of the core clock gene *bmal1* influences its effects on aging and survival. *Sci Transl Med.* (2016) 8:324ra16. doi: 10.1126/scitranslmed.aad3305
53. Zhang Y, Fang B, Emmett MJ, Damle M, Sun Z, Feng D, et al. Discrete functions of nuclear receptor Rev-ErbB1; couple metabolism to the clock. *Science.* (2015) 348:1488–92. doi: 10.1126/science.aab3021
54. Lanier LL. Nk cell receptors. *Annu Rev Immunol.* (1998) 16:359–93. doi: 10.1146/annurev.immunol.16.1.359
55. Posch PE, Hurley CK. Chapter 39 - Histocompatibility: Hla and other systems. In: Porwit A, McCullough J, Erber WN, editors. *Blood and Bone Marrow Pathology (Second Edition)*. Edinburgh: Churchill Livingstone (2011). p. 641–76. doi: 10.1016/B978-0-7020-3147-2.00039-0
56. Kollnberger S, Chan A, Sun M-Y, Ye Chen L, Wright C, di Gleria K, et al. Interaction of Hla-B27 homodimers with Kir3dl1 and Kir3dl2, unlike Hla-B27 heterotrimers, is independent of the sequence of bound peptide. *Eur J Immunol.* (2007) 37:1313–22. doi: 10.1002/eji.200635997
57. Ballek O, Valečka J, Dobešová M, Broučková A, Manning J, Rehulka P, et al. Tcr triggering induces the formation of lck-rack1-actinin-1 multiprotein network affecting lck redistribution. *Front Immunol.* (2016) 7:449. doi: 10.3389/fimmu.2016.00449
58. Jiang Y-p, Peng Y-q, Wang L, Qin J, Zhang Y, Zhao Y-z, et al. Rna-sequencing identifies differentially expressed genes in T helper 17 cells in peritoneal fluid of patients with endometriosis. *J Reproduct Immunol.* (2022) 149:103453. doi: 10.1016/j.jri.2021.103453
59. Qiu G, Liu J, Cheng Q, Wang Q, Jing Z, Pei Y, et al. Impaired autophagy and defective T cell homeostasis in mice with T cell-specific deletion of receptor for activated C kinase 1. *Front Immunol.* (2017) 8:575. doi: 10.3389/fimmu.2017.00575
60. Osborne DG, Piotrowski JT, Dick CJ, Zhang J-S, Billadeau DD. Snx17 affects T Cell activation by regulating Tcr and integrin recycling. *J Immunol.* (2015) 194:1402734. doi: 10.4049/jimmunol.1402734
61. Lopez BI, Santiago KG, Lee D, Ha S, Seo K. Rna sequencing (Rna-Seq) based transcriptome analysis in immune response of holstein cattle to killed vaccine against bovine viral diarrhoea virus type 1. *Animals.* (2020) 10:344. doi: 10.3390/ani10020344
62. McGill JL, Rusk RA, Guerra-Maupome M, Briggs RE, Sacco RE. Bovine gamma delta T cells contribute to exacerbated Il-17 production in response to co-infection with bovine Rsv and mannheimia haemolytica. *PLoS ONE.* (2016) 11:e0151083. doi: 10.1371/journal.pone.0151083
63. Ma WT, Yao XT, Peng Q, Chen DK. The protective and pathogenic roles of Il-17 in viral infections: friend or foe? *Open Biol.* (2019) 9:190109. doi: 10.1098/rsob.190109
64. Merle NS, Church SE, Fremereaux-Bacchi V, Roumenina LT. Complement system part i – molecular mechanisms of activation and regulation. *Front Immunol.* (2015) 6:262. doi: 10.3389/fimmu.2015.00262
65. Ling M, Murali M. Analysis of the complement system in the clinical immunology laboratory. *Clin Lab Med.* (2019) 39:579–90. doi: 10.1016/j.cl.2019.07.006
66. Kurtovic L, Beeson JG. Complement factors in Covid-19 therapeutics and vaccines. *Trends Immunol.* (2021) 42:94–103. doi: 10.1016/j.it.2020.12.002
67. Kim YJ, Kim KH, Ko EJ, Kim MC, Lee YN, Jung YJ, et al. Complement C3 plays a key role in inducing humoral and cellular immune

- responses to influenza virus strain-specific hemagglutinin-based or cross-protective M2 extracellular domain-based vaccination. *J Virol.* (2018) 92:e00969–18. doi: 10.1128/JVI.00969-18
68. Carroll MC. The complement system in regulation of adaptive immunity. *Nat Immunol.* (2004) 5:981–6. doi: 10.1038/ni1113
69. Molina H, Kinoshita T, Webster CB, Holers VM. Analysis of C3b/C3d binding sites and factor I cofactor regions within mouse complement receptors 1 and 2. *J Immunol.* (1994) 153:789–95.
70. Kopf M, Abel B, Gallimore A, Carroll M, Bachmann MF. Complement component C3 promotes T-cell priming and lung migration to control acute influenza virus infection. *Nat Med.* (2002) 8:373–8. doi: 10.1038/nm0402-373
71. Salehen Na, Stover C. The role of complement in the success of vaccination with conjugated vs. unconjugated polysaccharide antigen. *Vaccine.* (2008) 26:451–9. doi: 10.1016/j.vaccine.2007.11.049
72. Geering B, Stoeckle C, Rožman S, Oberson K, Benarafa C, Simon H-U. Dapk2 positively regulates motility of neutrophils and eosinophils in response to intermediary chemoattractants. *J Leukoc Biol.* (2014) 95:293–303. doi: 10.1189/jlb.0813462
73. Ni X, Wang Y, Wang P, Chu C, Xu H, Hu J, et al. Death associated protein kinase 2 suppresses T-B interactions and Gc formation. *Mol Immunol.* (2020) 128:249–57. doi: 10.1016/j.molimm.2020.10.018
74. Kim H, Dickey L, Stone C, Jafek JL, Lane TE, Tantin D, et al. Cell-selective deletion of Oct1 protects animals from autoimmune neuroinflammation while maintaining neurotropic pathogen response. *J Neuroinflammation.* (2019) 16:133. doi: 10.1186/s12974-019-1523-3
75. Shakya A, Goren A, Shalek A, German CN, Snook J, Kuchroo VK, et al. Oct1 and Oca-B are selectively required for Cd4 memory T cell function. *J Exp Med.* (2015) 212:2115–31. doi: 10.1084/jem.20150363
76. Hwang SS, Kim LK, Lee GR, Flavell RA. Role of Oct-1 and partner proteins in T cell differentiation. *Biochim Biophys Acta.* (2016) 1859:825–31. doi: 10.1016/j.bbagr.2016.04.006
77. Prado DS, Cattley RT, Shipman CW, Happe C, Lee M, Boggess WC, et al. Synergistic and additive interactions between receptor signaling networks drive the regulatory T cell versus T helper 17 cell fate choice. *J Biol Chem.* (2021) 297:101330. doi: 10.1016/j.jbc.2021.101330
78. Gao Y, Zhang X, Wang Z, Qiu Y, Liu Y, Shou S, et al. The contribution of neuropilin-1 in the stability of Cd4+Cd25+ regulatory T cells through the Tgf- $\beta$ /smads signaling pathway in the presence of lipopolysaccharides. *Immun Inflamm Dis.* (2022) 10:143–54. doi: 10.1002/iid3.551
79. Ran Y, Zhang J, Liu LL, Pan ZY, Nie Y, Zhang HY, et al. Autoubiquitination of trim26 links Tbk1 to nemo in Rlr-mediated innate antiviral immune response. *J Mol Cell Biol.* (2016) 8:31–43. doi: 10.1093/jmcb/mjv068
80. Huang H, Sharma M, Zhang Y, Li C, Liu K, Wei J, et al. Expression profile of porcine Trim26 and its inhibitory effect on interferon- $\beta$  production and antiviral response. *Genes.* (2020) 11:1226. doi: 10.3390/genes11101226
81. Zhao J, Cai B, Shao Z, Zhang L, Zheng Y, Ma C, et al. Trim26 positively regulates the inflammatory immune response through k11-linked ubiquitination of tab1. *Cell Death Differ.* (2021) 28:3077–91. doi: 10.1038/s41418-021-00803-1
82. Dargaud Y, Scoazec JY, Wielders SJH, Trzeciak C, Hackeng TM, Négrier C, et al. Characterization of an autosomal dominant bleeding disorder caused by a thrombomodulin mutation. *Blood.* (2015) 125:1497–501. doi: 10.1182/blood-2014-10-604553
83. Adams TE, Huntington JA. Thrombin-cofactor interactions. *Arterioscler Thromb Vasc Biol.* (2006) 26:1738–45. doi: 10.1161/01.ATV.0000228844.65168.d1
84. Millar DG, Garza KM, Odermatt B, Elford AR, Ono N, Li Z, et al. Hsp70 promotes antigen-presenting cell function and converts T-Cell tolerance to autoimmunity in vivo. *Nat Med.* (2003) 9:1469–76. doi: 10.1038/nm962
85. Castellino F, Boucher PE, Eichelberg K, Mayhew M, Rothman JE, Houghton AN, et al. Receptor-mediated uptake of antigen/heat shock protein complexes results in major histocompatibility complex class I antigen presentation via two distinct processing pathways. *J Exp Med.* (2000) 191:1957–64. doi: 10.1084/jem.191.11.1957
86. Ishii T, Udono H, Yamano T, Ohta H, Uenaka A, Ono T, et al. Isolation of Mhc class I-restricted tumor antigen peptide and its precursors associated with heat shock proteins Hsp70, Hsp90, and Gp96. *J Immunol.* (1999) 162:1303–9.
87. Asea A, Kraeft SK, Kurt-Jones EA, Stevenson MA, Chen LB, Finberg RW, et al. Hsp70 stimulates cytokine production through a Cd14-dependant pathway, demonstrating its dual role as a chaperone and cytokine. *Nat Med.* (2000) 6:435–42. doi: 10.1038/74697
88. Ambade A, Catalano D, Lim A, Mandrekar P. Inhibition of heat shock protein (molecular weight 90 Kda) attenuates proinflammatory cytokines and prevents lipopolysaccharide-induced liver injury in mice. *Hepatology.* (2012) 55:1585–95. doi: 10.1002/hep.24802
89. Ambade A, Catalano D, Lim A, Kopoyan A, Shaffer SA, Mandrekar P. Inhibition of heat shock protein 90 alleviates steatosis and macrophage activation in murine alcoholic liver injury. *J Hepatol.* (2014) 61:903–11. doi: 10.1016/j.jhep.2014.05.024
90. Lin L, Pan S, Zhao J, Liu C, Wang P, Fu L, et al. Hspd1 Interacts with Irf3 to facilitate interferon-beta induction. *PLoS ONE.* (2014) 9:e114874. doi: 10.1371/journal.pone.0114874
91. Mo Z, Zhang S, Zhang S. A novel signature based on mtorc1 pathway in hepatocellular carcinoma. *J Oncol.* (2020) 2020:8291036. doi: 10.21203/rs.3.rs-18272/v1
92. Cwiklinska H, Cichalewska-Studzinska M, Selmaj KW, Mycko MP. The heat shock protein Hsp70 promotes Th17 genes' expression via specific regulation of microRNA. *Int J Mol Sci.* (2020) 21:2823. doi: 10.3390/ijms21082823
93. Yang Y, Xia J, Yang Z, Wu G, Yang J. The abnormal level of Hsp70 is related to Treg/Th17 imbalance in pcos patients. *J Ovarian Res.* (2021) 14:155. doi: 10.1186/s13048-021-00867-0
94. Kim BK, Park M, Kim JY, Lee KH, Woo SY. Heat shock protein 90 is involved in Il-17-mediated skin inflammation following thermal stimulation. *Int J Mol Med.* (2016) 38:650–8. doi: 10.3892/ijmm.2016.2627
95. Baldwin CL, Damani-Yokota P, Yirsaw A, Loonie K, Teixeira AF, Gillespie A. Special features of T $\gamma$ 8 T cells in ruminants. *Mol Immunol.* (2021) 134:161–9. doi: 10.1016/j.molimm.2021.02.028
96. Houchins JP, Yabe T, McSherry C, Bach FH. DNA sequence analysis of Nkg2, a family of related cdna clones encoding type ii integral membrane proteins on human natural killer cells. *J Exp Med.* (1991) 173:1017–20. doi: 10.1084/jem.173.4.1017
97. Guzman E, Birch JR, Ellis SA. Cattle mic is a ligand for the activating Nk Cell receptor Nkg2d. *Vet Immunol Immunopathol.* (2010) 136:227–34. doi: 10.1016/j.vetimm.2010.03.012
98. Blunt MD, Vallejo Pulido A, Fisher JG, Graham LV, Doyle AD, Fulton R, et al. Kir2ds2 expression identifies Nk cells with enhanced anticancer activity. *J Immunol.* (2022) 209:379–90. doi: 10.4049/jimmunol.2101139
99. Closa L, Xicoy B, Zamora L, Estrada N, Colomer D, Herrero MJ, et al. Natural killer cell receptors and ligand variants modulate response to tyrosine kinase inhibitors in patients with chronic myeloid leukemia. *Hla.* (2022) 99:93–104. doi: 10.1111/tan.14515
100. Mofteh NH, El-Barbary RA, Rashed L, Said M. Ulbp3: a marker for alopecia areata incognita. *Arch Dermatol Res.* (2016) 308:415–21. doi: 10.1007/s00403-016-1652-9
101. Sutherland CL, Rabinovich B, Chalupny NJ, Brawand P, Miller R, Cosman D. Ulbps, human ligands of the Nkg2d receptor, stimulate tumor immunity with enhancement by Il-15. *Blood.* (2006) 108:1313–9. doi: 10.1182/blood-2005-11-011320
102. Mou X, Zhou Y, Jiang P, Zhou T, Jiang Q, Xu C, et al. The regulatory effect of Ul-16 binding protein-3 expression on the cytotoxicity of Nk cells in cancer patients. *Sci Rep.* (2014) 4:6138. doi: 10.1038/srep06138
103. Bassi PB, Araujo FF, Garcia GC, Costa ESMF, Bittar ER, Bertonha CM, et al. Haematological and immunophenotypic evaluation of peripheral blood cells of cattle naturally infected with bovine papillomavirus. *Vet J.* (2019) 244:112–5. doi: 10.1016/j.tvjl.2018.12.004
104. Hamilton CA, Mahan S, Entrican G, Hope JC. Interactions between natural killer cells and dendritic cells favour T helper1-type responses to bcg in calves. *Vet Res.* (2016) 47:85. doi: 10.1186/s13567-016-0367-4
105. De Beuckelaer A, Pollard C, Van Lint S, Roose K, Van Hoecke L, Naessens T, et al. Type I interferons interfere with the capacity of Mrna lipoplex vaccines to elicit cytolytic T cell responses. *Mol Ther.* (2016) 24:2012–20. doi: 10.1038/mt.2016.161
106. Zhong C, Liu F, Hajnik RJ, Yao L, Chen K, Wang M, et al. Type I interferon promotes humoral immunity in viral vector vaccination. *J Virol.* (2021) 95:e0092521. doi: 10.1128/JVI.00925-21
107. Ye L, Ohnemus A, Ong LC, Gad HH, Hartmann R, Lycke N, et al. Type I and type iii interferons differ in their adjuvant activities for influenza vaccines. *J Virol.* (2019) 93:e01262–19. doi: 10.1128/JVI.01262-19
108. Crow MK, Ronnblom L. Type I interferons in host defence and inflammatory diseases. *Lupus Sci Med.* (2019) 6:e000336. doi: 10.1136/lupus-2019-000336

109. Tizioto PC, Kim J, Seabury CM, Schnabel RD, Gershwin LJ, Van Eenennaam AL, et al. Immunological response to single pathogen challenge with agents of the bovine respiratory disease complex: an rna-sequence analysis of the bronchial lymph node transcriptome. *PLoS ONE*. (2015) 10:e0131459. doi: 10.1371/journal.pone.0131459
110. Behura SK, Tizioto PC, Kim J, Grupioni NV, Seabury CM, Schnabel RD, et al. Tissue tropism in host transcriptional response to members of the bovine respiratory disease complex. *Sci Rep*. (2017) 7:17938. doi: 10.1038/s41598-017-18205-0
111. Johnston D, Earley B, McCabe MS, Kim J, Taylor JF, Lemon K, et al. Messenger Rna biomarkers of bovine respiratory syncytial virus infection in the whole blood of dairy calves. *Sci Rep*. (2021) 11:9392. doi: 10.1038/s41598-021-88878-1
112. Scott MA, Woolums AR, Swiderski CE, Perkins AD, Nanduri B. Genes and regulatory mechanisms associated with experimentally-induced bovine respiratory disease identified using supervised machine learning methodology. *Sci Rep*. (2021) 11:22916. doi: 10.1038/s41598-021-02343-7